PL-TR-96-2249

REGIONAL DISCRIMINATION STUDIES

Chris Hayward
Eugene Herrin
G. G. Sorrell
Ileana Tibuleac

Southern Methodist University
Dallas, TX 75275

April 1996

Scientific Report No. 1

PHILLIPS LABORATORY
Directorate of Geophysics
AIR FORCE MATERIEL COMMAND
HANSCOM AFB, MA 01731-3010

SPONSORED BY
Advanced Research Projects Agency (DoD)
Nuclear Monitoring Research Office
ARPA ORDER No. 0325

MONITORED BY
Phillips Laboratory
CONTRACT No. F19628-95-C-0184

The views and conclusions contained in this document are those of the authors and should not be interpreted as representing the official policies, either express or implied, of the Air Force or U.S. Government.

This technical report has been reviewed and is approved for publication.

DELAINE R. REITER
Contract Manager
Earth Sciences Division

JAMES F. LEWKOWICZ
Director
Earth Sciences Division

This report has been reviewed by the ESD Public Affairs Office (PA) and is releasable to the National Technical Information Service (NTIS).

Qualified requestors may obtain copies from the Defense Technical Information Center. All others should apply to the National Technical Information Service.

If your address has changed, or you wish to be removed from the mailing list, or if the addressee is no longer employed by your organization, please notify PL/IM, 29 Randolph Road, Hanscom AFB, MA 01731-3010. This will assist us in maintaining a current mailing list.

Do not return copies of this report unless contractual obligations or notices on a specific document requires that it be returned.

DISCLAIMER NOTICE

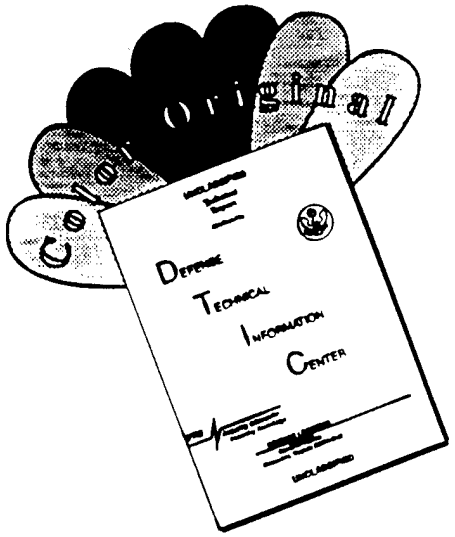

THIS DOCUMENT IS BEST QUALITY AVAILABLE. THE COPY FURNISHED TO DTIC CONTAINED A SIGNIFICANT NUMBER OF COLOR PAGES WHICH DO NOT REPRODUCE LEGIBLY ON BLACK AND WHITE MICROFICHE.

REPORT DOCUMENTATION PAGE

Form Approved
OMB No. 0704-0188

1. AGENCY USE ONLY (Leave blank)	2. REPORT DATE	3. REPORT TYPE AND DATES COVERED
	April 1996	Scientific No. 1

4. TITLE AND SUBTITLE
Regional Discrimination Studies

5. FUNDING NUMBERS
PE 62301F
PR NM95 TAGM
WU AD
Contract F19628-95-C-0184

6. AUTHOR(S)
Chris Hayward, Eugene Herrin
G.G. Sorrell, Ileana Tibuleac

7. PERFORMING ORGANIZATION NAME(S) AND ADDRESS(ES)
Southern Methodist University
Dallas, TX 75275-0395

8. PERFORMING ORGANIZATION REPORT NUMBER

9. SPONSORING/MONITORING AGENCY NAME(S) AND ADDRESS(ES)
Phillips Laboratory
29 Randolph Road
Hanscom AFB, MA 01731-3010

Contract Manager: Delaine Reiter/GPE

10. SPONSORING/MONITORING AGENCY REPORT NUMBER
PL-TR-96-2249

11. SUPPLEMENTARY NOTES

12a. DISTRIBUTION/AVAILABILITY STATEMENT
Approved for public release; distribution unlimited

12b. DISTRIBUTION CODE

13. ABSTRACT *(Maximum 200 words)*

Part 1 describes TXAR in detail. The first Alpha-type station proposed by the GSE in 1993 is the Texas Experimental Seismic System (TEXESS), now designated TXAR, located at Lajitas, Texas, and operated by SMU during GSETT-1 and GSETT-2. Part 2 describes the results of the study of 144 events recorded at TXAR. The correlation method used allows the analysis of weak regional to teleseismic events and the identification of successive phases for each event. Corrected phase velocities show P_n first arrivals come to TXAR from as far as 2000 km. Events at greater distances have mantle P waves as first arrivals. Part 3 describes construction of a new Ground Truth Data Base using regional events from a variety of sources. Known sources include mine explosions, normal earthquakes, earthquake swarms, and very shallow earthquakes induced by hydrocarbon production. These induced earthquakes are only 1 to 4 km deep and have been observed with magnitudes ranging from 1.0 to 4.6. We believe all events in the Permian Basin of Texas to the northeast of TXAR are induced and are associated with oil and gas fields. Part 4 are the Acknowledgments required by the contract.

14. SUBJECT TERMS	15. NUMBER OF PAGES
Long period seismometers Calibration Studies Ground Truth Data Base	62
	16. PRICE CODE

17. SECURITY CLASSIFICATION OF REPORT	18. SECURITY CLASSIFICATION OF THIS PAGE	19. SECURITY CLASSIFICATION OF ABSTRACT	20. LIMITATION OF ABSTRACT
Unclassified	Unclassified	Unclassified	SAR

CONTENTS

CONTENTS

CONTENTS

1. TXAR: THE PROTOTYPE ALPHA ARRAY OF THE NEW IMPROVED GLOBAL SEISMIC SYSTEM

Chris Hayward

1.1 INTRODUCTION

GSETT-2 misassociations by four independent EIDC's, which published four event bulletins, resulted in a high percentage of hypocenter mislocations. As a result, the GSE proposed in 1993 to establish a new improved global system consisting of one IDC, which would publish one bulletin, and a core network, termed an Alpha Network, of 50 stations, primarily arrays. Data from the Alpha Network would be augmented by data from a Beta Network of greater than 60 regional stations and a Gamma Network of local stations. The first Alpha-type station was the Texas Experimental Seismic System (TEXESS), now designated TXAR, which was located at the Lajitas, Texas, site (LTX) operated by SMU during GSETT-1 and GSETT-2. Two more Alpha-type stations are planned for Egypt and Pakistan. This new improved global system will be evaluated by the third international test, GSETT-3, beginning 1 January 1995.

SMU began research on mini-array technology in 1991 under Contract # MDA 972-89-C-0054, and was awarded Contract # F19628-93-C-0057 to install TEXESS on 5 April 1993. The proposed array design was along the lines of a GSE Alpha Station mentioned above. TEXESS was installed by SMU personnel at their LTX site the week of 22 August 1993, and the first event was a local recorded on 31 August. The array, having an aperture of 4 km, consists of nine sensor sites, which includes a central three-component, short-period seismometer installation in a vault at the hub, and eight vertical short-period seismometer installations in surrounding boreholes. In addition to the short-period instrumentation at the hub, a posthole K-S54000 long-period seismometer, owned by SMU, was installed in a shallow borehole. The term *posthole* was coined because the K-S54000 is slimmer than the K-S36000 and is installed in a shallow hole without a hole lock in such a manner that it can be leveled manually rather than remotely.

The LTX site has been operated as a remote telemetered seismic station by Southern Methodist University's Department of Geological Sciences personnel under DARPA Contract # MDA 972-88-K-001 since 1980. Chosen for its remote location far from common cultural and seismic noise sources, the Lajitas area is an ideal location for testing state-of-the-art seismic equipment and techniques. Except for a few times a year, when the area receives visitors from movie companies filming nearby, or from participants in the world-class chili cookoff, it holds the title of "The world's quietest seismic site" with a mean ambient background noise of 0.8 nm/sec at 1 Hz. Upon integrating the velocity by dividing by $2\pi f$, one obtains a displacement of .127 nm or 1.3 Angstom, which is pretty quiet.

This paper covers historical background, array geometry, testing, borehole drilling, training, element description, electronics installation, array hub and controller, short-period seismometer installation, broadband element installation, and accessing TXAR "Home Page."

1.2 HISTORY

In early 1992 after completing the 21-element GERESS array in Germany, we began to thing about reducing the costs of installation and operation of a telemetered seismic array without sacrificing the performance. Installing GERESS was a major planning and construction project involving seismometer-vault excavation, miles of trenching for cables and conduits, and substantial data communication engineering.

At GERESS, vault evacuation, cable trenching, and conduit installation were major expenses. Not only was the construction itself expensive, but substantial managerial time was required to resolve environmental concerns caused by cutting and trenching operations. At the time though, there was no alternative to these operations.

As work on GERESS neared completion, there were several informal discussions with other academic seismologists who had experimented with other installation methods. The GPS, Global Positioning System consisting of a constellation of 24 satellites orbiting the earth at a very high altitude, was

almost complete making it possible to get world time several times per day. And reasonably priced commercial GPS clocks and receivers were being developed. By using GPS receivers at each site, there would be no need for radio-cable links from the hub.

Researchers examining the performance of the NORESS and-GERESS-style arrays were beginning to question the need for 21 elements for all signals in quiet locations. In some cases, array performance was improved by dropping one or more elements. It appeared that choosing a few good sites might be more important than precise geometry control.[1]

These discussions and developments led to the consideration of finding an inexpensive method of installing a vault, which is traditionally blasted from hard rock; finding some way of avoiding the expense of long cable runs and the risk of lightning strikes; and finding a method of installing the equipment quickly. The search wasn't unique because other seismologists had been deploying temporary and permanent networks of seismic stations with elements having some of these characteristics. In our case though, we wished to design an array system from the start that would be capable of unlimited seismic performance.

Our experience in system development led us to conclude that the prototype would have to be tested and refined at the Lajitas site for over one year prior to being considered an operational design.

1.3 ARRAY GEOMETRY

The initial array design was to be 8 short-period vertical seismometers arranged in concentric 4-km and 1-km diameter circles plus a central 3-component seismometer in a standard vault. The rugged topography and site access controlled the permissible locations. As a result, some elements were moved from their ideal locations. The final array geometry and site designations are shown in Figure 1.

---

[1] In 1971, LASA performance was improved after elements were removed for installation at NORSOR.18

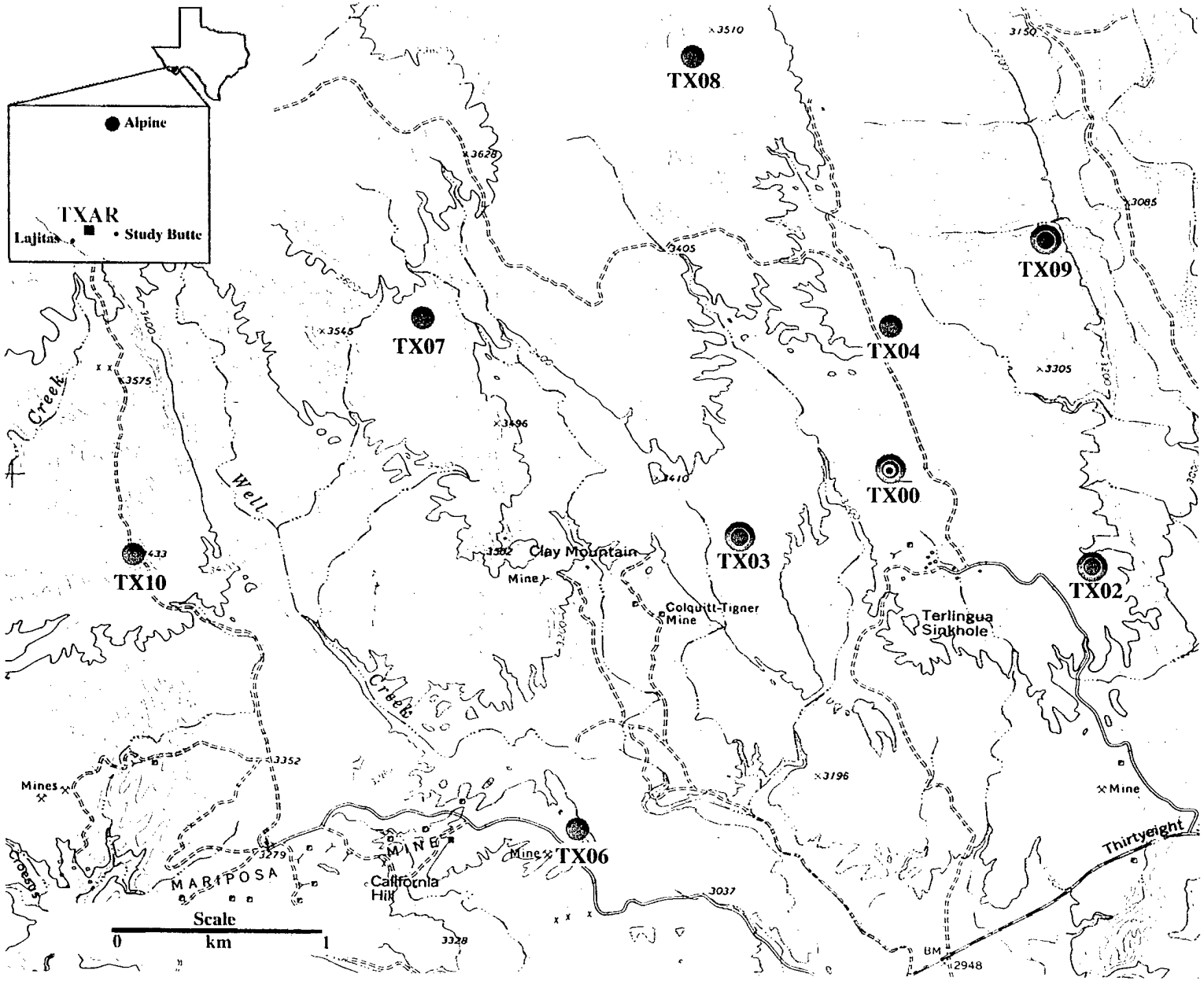

Figure 1. Map of TXAR with site designations.

Massive Cretaceous limestone crops out on the surface -- there is no soil -- making trenching and excavation operations prohibitably expensive. All elements were therefore designed to use radio telemetry and be self-powered. This also allowed additional elements to be added, or noisy elements to be located at little cost.[2] The requirement for radio telemetry using VHF frequencies imposed one additional restriction on the geometry. Elements were required to be within VHF transmission range of the concentrator and controller at the hub. While repeaters were a possibility, they would have added additional complexity to the design.

1.4 TESTING AT THE LTX SITE

1.4.1 LTX Site

The principal facility at the LTX site is a 20x8 foot trailer, which serves as an onsite laboratory and sleeping quarters. During early testing and installation, a full set of workstations and processing equipment was installed in the trailer. The workstation running a real time data acquisition and viewing system was used to QC the data and perform instrument tests without interrupting the archival flow of data back to SMU. At other times, the trailer functioned as a classroom, an office, and dining quarters.

Before the installation of the array, extensive tests were performed using the LTX systems, which consisted of three-component short-period and broadband seismometers. At the time, a 24-bit, 6-channel recording system, developed for GSETT-2, was delivering continuous seismic data to SMU's lab in Dallas. It also had the capability of recording 7 additional 16-bit channels. LTX was the prototype GSETT-2 seismograph system.

1.4.2 Noise Tests

As a first experiment, a small 3-element mini-array was deployed using Spirl-4 cables. Vertical sensors were installed in 2-foot-deep vaults located about 1/4 mile from the trailer. Data collected during this experiment confirmed earlier

[2] After analysis of data, one site was moved that was unusually noisy due to proximity to a road and powerline. In addition, another element was added to handle an additional sensor at the hub.

results that under quiet conditions, even at such short distances, the background noise showed little correlation.

The experiment also demonstrated the danger of cabled systems at LTX. A nearby summer thunderstorm induced large currents in the cables, blowing components off of the surge-protection boards and then fusing components in the power supply, analog preamps, and portions of the digital circuits. Induced currents from lightning would continue to be a problem through much of the testing program.

1.4.3 Testing the First Telemetered Element

Initial testing was made with one remote element radio telemetered back to the hub. During this phase, various combinations of antenna were tried to improve the immunity to noise. The yagi antenna shown in Figure 2 was subsequently found unnecessary.

Initial installation and tests were done with one 3-component digitizer and vault instrument on cable and one borehole vault on digital radio telemetry. The vault instrument was compared with a collocated GSETT-2 system that had been operational for a number of years and had undergone extensive testing and development.

The small size and low power of the central controller allows it to be backed up with a small set of 12-volt batteries to handle any short-term power outages. for use during the tests, the radio and controller were first used outside, then they were moved next to the workstation in the trailer.

By comparing the performance of the cabled-vault element with the telemetered borehole element, the effects of radio telemetry on the data reliability and the performance of the borehole vault during periods of high wind could be determined. During this stage of development, a number of minor changes were made to the software, firmware on the digitizers and communications controller, and hardware to improve the performance and assist in field diagnostics.

1.5 DRILLING THE HOLES

The first four holes at LTX were drilled in 1991, and the remaining four were drilled during the week of 16 May 1993. As mentioned previously, access to the sites was one of the principal restrictions that had to be considered; the other was radio telemetry line-of-sight. Location and access had been scouted by SMU personnel during a prior trip to LTX. A two-man contract crew drilled the holes with conventional water well equipment.

While air drilling in limestone can be a dusty operation, it causes far less impact on the surrounding countryside than the more conventional vault excavation using dynamite. The holes were drilled oversized so there would be sufficient clearage to cement the casing from the surface down. Once a hole was drilled and before the casing was set, several feet of cement grout was poured into the bottom of the hole to form the "floor" of the borehole vault. The casing was then carefully lowered into the slurry, plumbed, and then left to set, usually overnight. Cementing was completed by pouring a slurry around the outside of the casing until the entire length is cemented. The top of the casing was then capped to seal out rainwater and rocks thrown by children.

Most of the boreholes were drilled to a depth of 20 feet, but one was drilled to 40 feet to determine if the same technique described above could be used in a deeper hole. It was found that seismometer installation in the deeper hole was no more difficult than in the shallow holes.

1.6 TRAINING CLASSES AND FAMILIARIZATION

Successful installation of the GS-13 seismometer requires a special procedure for borehole installation. Instead of adjusting instrument level and free period after installation, it must be preset prior to installation in the borehole. During the site preparation for the array, a training class was held to demonstrate the technique and familiarize seismologists and technicians from Pakistan with the procedure. Training included both instructions in the software and analysis of the data at SMU as well as installation field training

at LTX. The visiting personnel learned the methods needed to completely install a system in Pakistan and to diagnose common problems.

1.7 ELEMENT DESCRIPTION

The prototype array element shown in Figures 2 and 3 includes the following;

1. A self-contained solar-charged power supply
2. A GPS time-keeping system
3. A digital radio modem and associated antenna
4. A 24-bit digital data acquisition system
5. A low noise seismometer preamp
6. A high-gain vertical seismometer

The two 40-watt solar panels provide power to charge lead-acid batteries within the enclosure below the panels. The panels produce sufficient power to run all the equipment within one hour of sunrise. A short time later, there is sufficient excess power to charge the batteries. Tests have demonstrated that the batteries supply enough power to run the system continuously for one week without any solar power and can recover within a full day of sunshine.

The two deep-cycle, 6-volt, golf-cart batteries supply power tot the electronics at each site. These batteries gave a capacity in excess of 1200 watt-hours. During later maintenance, these were replaced with more easily obtained high-capacity automotive battery.

Mounted above the antenna is a GPS receiver (see Figure 1-2) that provides precise world time and location. Location is appended to state-of-health information. unambiguously identifying each data stream that has proved particularly useful when coordination between the field activities and data recording is difficult. Testes of the system indicate that the ample synchronization and timing accuracy of the system is better than two microseconds from world time. Thus, samples from two different elements are always within 4 microseconds from each other.

The rest of the electronics at the site (see Figure 1-3) is within the borehole where it is protected from daily temperature extremes and is isolated from

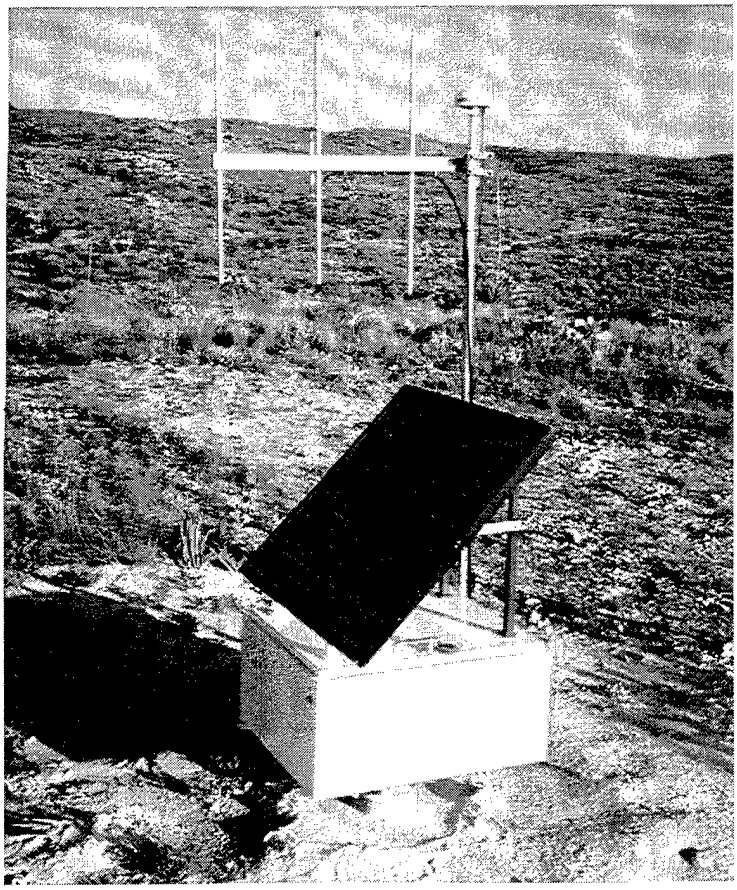

Figure 2. Prototype solar-power array and antenna.

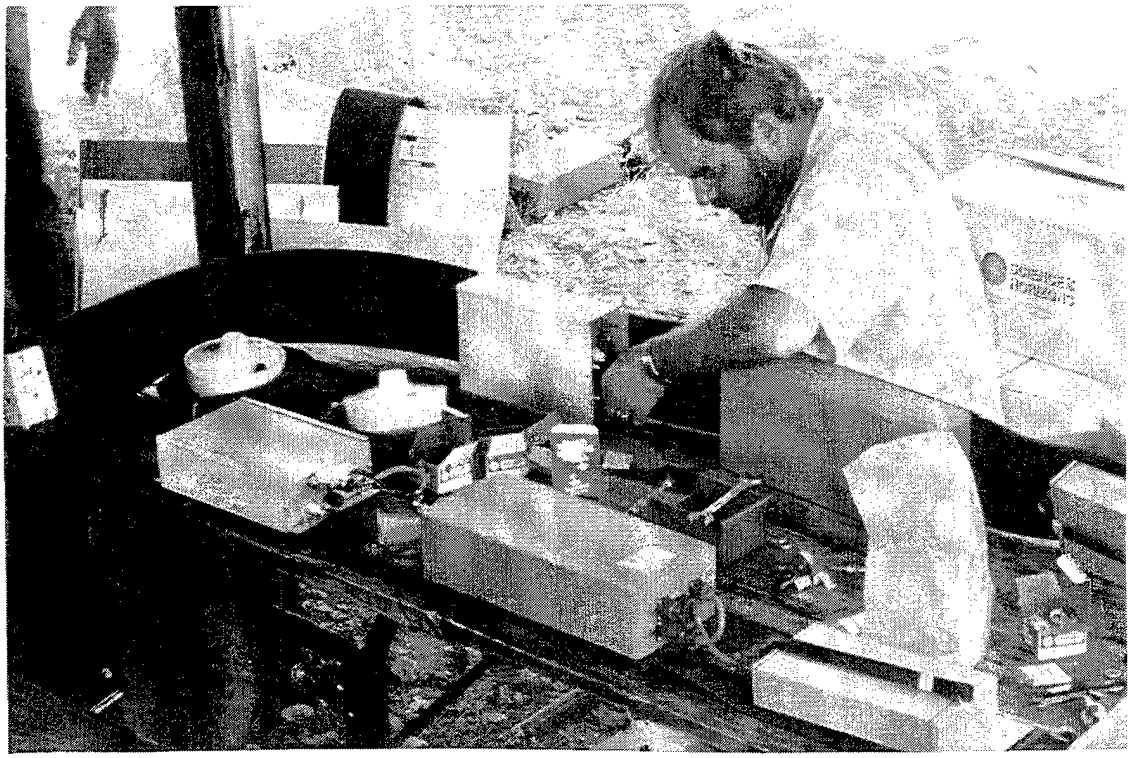

Figure 3. Carrier strip and electronics.

corrosive gases that may escape from the batteries in the enclosure, which is well vented.

1.8 ELECTRONICS INSTALLATION

Once the boreholes were completed and the grout was cured, the sites were ready for the electronics-package installation. All the required items had been shipped from SMU. The heavy items such as batteries, boxes, and solar panels were shipped by motor freight while the electronics were shipped by air express. SMU technicians transported the seismometers from Dallas in the back of a light truck.

To install the equipment, a 4-person field crew assembled and physically installed the 9 sites in 7 working days. Once the equipment was installed, the crew rotated and 3 people remained an additional week to complete the configuration and initial checkout. Assembly of the electronics package requires a minimum of tools and expertise and is simple enough to complete in the field. All the borehole electronics packages were assembled in a few hours. The wellhead enclosures were completed the previous week.

Figure 3 shows the borehole strap or carrier strip and electronics. At the bottom of the strap is the preamp, then the digitizer, and then the radio modem. The small round units are the GPS clocks (?). The strap with the electronics is lowered into the borehole, and the wellhead enclosures are attached (see Figure 2). It required less than an hour at each site to complete the installation.

The electronics are usually preconfigured prior to installation such that the final configuration can be made from the hub. A laptop computer can record and display short segments of waveforms to verify instrument performance, digitizer performance, radio-circuit links, and instrument calibration. It also provides text (?) communication back to the recording site. This allows technicians to verify that an element is working prior to leaving the site.

1.9 ARRAY HUB AND CONTROLLER

The array remote operations facility (ROF) includes a satellite transmitter dish for the circuit back to SMU, a VHF antenna mounted on a telephone pole for the hub-to-element links, a standby-power system, and a building for the electronics. A single, four-element omnidirectional antenna at the hub receives data from all array elements, and transmits commands to each element. Only three VHF frequencies are used for the 9 RF linked elements. The antenna feeds two VHF radio modems connected to an array controller and data concentrator. The output of the concentrator feeds a single satellite circuit to SMU.

Equipment in the ROF includes the following:

1. Digital radio modems
2. Communications interface array controller
3. Satellite modem
4. Telephone
5. Dial modem
6. Uninterruptable power supply (UPS).

The communication controller polls each element on a command frequency and receives data on one of the two data frequencies. Messages are error-corrected, if needed, so that no data is lost due to short-transmission errors. Data are then compressed, blocked if needed, and transmitted by the satellite modem to the SMU data center where it is forwarded to clients.

The high-capacity UPS provides up to 4 hours of standby power from a small battery bank. A telephone connection directly to the UPS allows the monitoring of state-of-health for the power supply, power cycling of the equipment in emergencies, and warning of battery failure. Because commercial power at TXAR may frequently be out longer than a few hours, alternative means of powering the satellite transmitter must be available. The radios and communications controller are low enough power to be supplied from batteries if necessary.

For over one year, the hub was powered totally from a 400-watt, propane-fired thermoelectric generator (TEG). A large gas tank had to be refilled about every two months; however, the system was highly reliable and completely independent of commercial power. After installation of the full array, the TEG system was switched to the more economical UPS system.

A propane-fueled, D-C generator was installed to back up the UPS battery system. It is designed for unattended operation, with automatic alarms and shutdowns to prevent engine damage in the event of mechanical failure, and reminders for periodic maintenance. This system has been in operation at TXAR for over one year.

The motor-generator back up is capable of handling extended power outages. It also supplies sufficient power (3 Kw) to run one or more on-site workstations used during experiments. like the UPS, the generator also has the capability for remote state-of-health monitoring.

1.10 SHORT-PERIOD SEISMOMETER INSTALLATION

1.10.1 Adjusting Free Period And Leveling

The installation of the seismometer begins with the final adjustment of the instrument for free period and a level surface. The assumption was made that the floor surface of the borehole would be level because of the way the floor was poured. final adjustment of the free period is required to adjust for any changes that may have occurred during shipping or transport and to verify that all instruments are set exactly the same. Because the array sites are far from commercial power, it is convenient to setup the seismometers prior to moving the equipment to respective sites.

1.10.2 Cleaning Out A Borehole

Debris at the bottom of the holes were checked with a small telescope. Cement and water, respectively, accumulated in the bottom of a couple of holes. The cement was removed by large wads of sticky tape on the end of a pole, and the water was removed with a sponge tool.

1.10.3 Installation Procedures

Mating the casing to the well-head enclosure was done with a custom-threaded flange. A padlock and chain was used to secure the cover while the cement was curing for the site close to a well-traveled highway.

The enclosure is mounted to the well casing with 8 large bolts. One or more may be electrically connected to the casing to secure a good electrical ground. Once the box is installed, it forms a convenient structure for mounting a small winch used to lower the seismometer.

A dummy seismometer is lowered into the hole to gauge the depth. During installation, the seismometer is lowered by the winch within a foot of the bottom and then by hand the final foot. Lowering by winch avoids banging the seismometer against the side of the casing, while the final hand work allows a much gentler placement on the bottom of the hole.

1.10.4 Lowering The Seismometer

The seismometer is attached to the cable for lowering into the borehole. In order to lock the mass during this operation, a D-C current is applied to the main coil to force it against the stops. A volt meter and amp meter are used to monitor the operation to insure that the coil remains locked during the operation.

1.10.5 Checking Level

The biggest problem is getting enough light down at the bottom of the hole to read the level. A strong spotlight is useful. By examining the level on the top of the instrument through a small telescope, it is possible to determine if the instrument is level. On occasions, it is necessary to rotate the seismometer slightly to avoid irregularities on the floor. At this point, he seismometer is installed and the site is ready for the final electronics installation and configuration.

1.11 BROADBAND ELEMENT INSTALLATION

1.11.1 KS36000 Posthole Seismometer

Originally designed to be installed in 100-meter-deep boreholes, the KS36000 and subsequently the KS54000 are standard instruments used at sites across the world. By installing them in deep boreholes, the effect of wind noise is diminished at lower frequencies. The construction of a deep borehole and subsequent instrument installation is a complex, expensive operation. If a site is sufficiently quiet, or the longer periods are only of secondary interest, then a shallow posthole installation can provide substantial savings while still producing an instrument superior to most vault installations.

1.11.2 Borehole Installation

The posthole version of the instrument requires none of the complex remote leveling mechanisms and does not require a hole lock or the equipment to install it. It also does not require a winch or the leasing of expensive orientation equipment. In the event there is a problem, pulling the instrument is a simple operation that does not usually result in instrument damage. In fact, the instrument was pulled then reinstalled within a morning.

1.11.3 Sand Packing

Once the instrument is in place in the borehole, which is a 20-foot-deep, 9-in. diameter, cased hole. Fine sand is poured around the instrument to firmly couple it to the surrounding rock. It is mechanically leveled from the surface, which sets a practical limit on the depth of the borehole, with long rods. Once leveled, as observed from the output, additional sand is added.

1.12 TXAR HOME PAGE

Information about TXAR can be accessed on Internet via the World Wide Web at:
http://inge.css.gov:65123/WebIDC/About_TXAR/

1.13 CONCLUSIONS

Advancements in the TXAR design included the following:

1. The placement of seismometers and electronics in boreholes to greatly reduce construction costs for piers and vaults,
2. The use of solar power at each site rather than a central-power source,
3. The use of GPS receivers for time data at each seismometer site to replace central timing from the Hub,
4. The employment of radio links from seismometer sites to the Hub to replace cable links and associated construction costs,
5. The use of modular equipment to facilitate the installation and maintenance of the array.

The above advancements in array design reduced costs by over an order of magnitude when compared with GERESS. Cost per element at GERESS was $341,280 whereas cost per element at TXAR was $33,000. With improved digital instrumentation to assure undistorted phase information and time-domain processing, azimuthal deviations for test events have been reduced significantly. As a result, TXAR is better than either a single, three-component station or larger arrays. After 35 years, we're back to the original Geneva-type array, or, in the words of Yogi Berra, "it's *dèjá vu* all over again."

2. CALIBRATION STUDIES AT TXAR

Ileana Tibuleac and Eugene Herrin

2.1 ABSTRACT

Calibration studies at TXAR (Lajitas, Texas) used a modified version of the correlation method described by Cansi, Plantet and Massinon (1993) in order to estimate azimuth and horizontal phase velocity of 144 events for which USGS mb values were available. Modifications to the correlation method include the Fourier interpolation of the data by a factor of 8 to obtain a virtual sample rate of 320/sec, use of an L1 norm (least absolute deviation) to obtain estimates of the azimuth and phase velocity and a moving window display to indicate those portions of the waveform that show strongest correlation across the array.

Corrected phase velocities normally associated with Pn (less than 8.6 km/s) are generally seen for events at epicentral distance as far as 2000 km. For greater distances, upper mantle refracted first arrivals (P) with corrected phase velocities greater than 8.6 km/s are generally observed for epicentral distances beyond 1600 km. Phase identification is essential in order to select a suitable magnitude scale.

Based on the 144 well located events (USGS) and using the Denny, Taylor and Vergino (1987) formula, the most reliable magnitude estimates are as follows:
1. For horizontal phase velocity less than 8.6 km/sec:
mb(D)=log A + 2.4 (log D) - 3.95 + C with C=+0.3
2. For horizontal phase velocity greater than 8.6 km/sec:
mb(D)=log A + 2.4 (log D) - 3.95 + C with C=-0.50

The M-discontinuity beneath TXAR was determined to the first order to strike along an azimuth of 111 degrees (NW-SE) and dip 10 degrees to the northeast. This result is consistent with the tectonic setting for the area.

2.2 INTRODUCTION

Calibration is generally required in order to reduce bias in location and magnitude determinations at regional to near-teleseismic distances using seismic array data. Calibration is particularly important at TXAR (Lajitas, Texas) because the array is located near the boundary between two geophysically different regions, the Mid-Continent and the Basin and Range Provinces.

The main objective is to obtain sufficient calibration information so that TXAR can provide reliable single-array locations and magnitudes of regional to near-teleseismic events.

The bias in estimated back-azimuth and horizontal phase velocity resulting from crustal structure under TXAR must be corrected before making a single array location. A modified version of the correlation method described by Cansi, Plantet and Massinon (1993) was used to estimate back-azimuth and horizontal phase velocity of 144 events recorded at TXAR for which USGS m_b values were available. Azimuth residuals versus estimated back-azimuth were used to correct the back-azimuth, and the best fitting first order attitude for the M-discontinuity under TXAR was derived from the residuals using a method similar to those described by Niazi (1966) and Otsuka (1966). We used a velocity model of the crust modified from the iasp91 velocity model (IASPEI 1991 Seismological Tables) as follows: A 35 km thick crust with P velocity 6.5 km/sec and an uppermost mantle velocity of 8.04 km/sec.

The great complexity in P wave velocity structure in the western United States described by Herrin and Taggart (1962) is responsible for the lack of a generally accepted m_b (P_n) or m_b (P) formula in that region. Several formulas have been proposed by Richter (1958), Evernden (1967), Veith and Clawson (1972) and Denny, Taylor and Vergino (1987). Phase identification is essential in order to select a suitable magnitude scale. Various magnitude estimates, corresponding to previous proposed formulas, were made and compared to USGS m_b. The most reliable estimates were those that used the Denny, Taylor and Vergino (1987) formula.

2.3 DATA USED

The data set of regional and near teleseismic events is composed of 144 shallow and intermediate depth earthquakes (153 arrivals - both P_n and P were used for 9 events) recorded by the short period vertical seismometers at TXAR and located by NEIS, for a time period between January 1994 and August 1995. The epicentral distances of these events range from 227 to 4703 km and the magnitude, m_b (USGS), ranges from 2.7 to 6.6. The true and estimated azimuths for these events are shown in Figure 4.

2.4 ARRAY DATA PROCESSING

It was assumed that the propagation of the wave across the array can be modeled by a plane wave whose back-azimuth and horizontal speed are to be estimated. Conversely, one could estimate the magnitude and direction of the slowness vector. The digital array data from nine short-period, vertical sensors sampled at 40 sps were loaded into a MATLAB environment and data from excessively noisy channels were discarded. The waveforms were bandpass filtered in order to increase the signal-to-noise ratio. A 3.2 seconds window was selected and moved with a step of 0.125 seconds (5 sample points) through the waveforms. The arrival time differences between each pair of stations were determined by cross-correlations of the data from all channels in the chosen window.

Modifications to the correlation method of Cansi et al (1993) include the Fourier interpolation of the data by a factor of 8 to obtain a virtual sample rate of 320 sps, the minimization of the L1 norm (least absolute deviation) to obtain estimates of the azimuth and horizontal phase velocity and the use of a moving window display to indicate those portions of the waveforms that show strongest correlation across the array.

Using Fourier interpolated data, a complete correlation matrix was computed. By calculating the lag times of the maxima of the cross-correlation functions, a complete lag matrix was also computed. This matrix must be skew symmetric. In the absence of noise and computational errors the lag matrix is Toeplitz. The lag matrix was corrected for differences in stations elevations

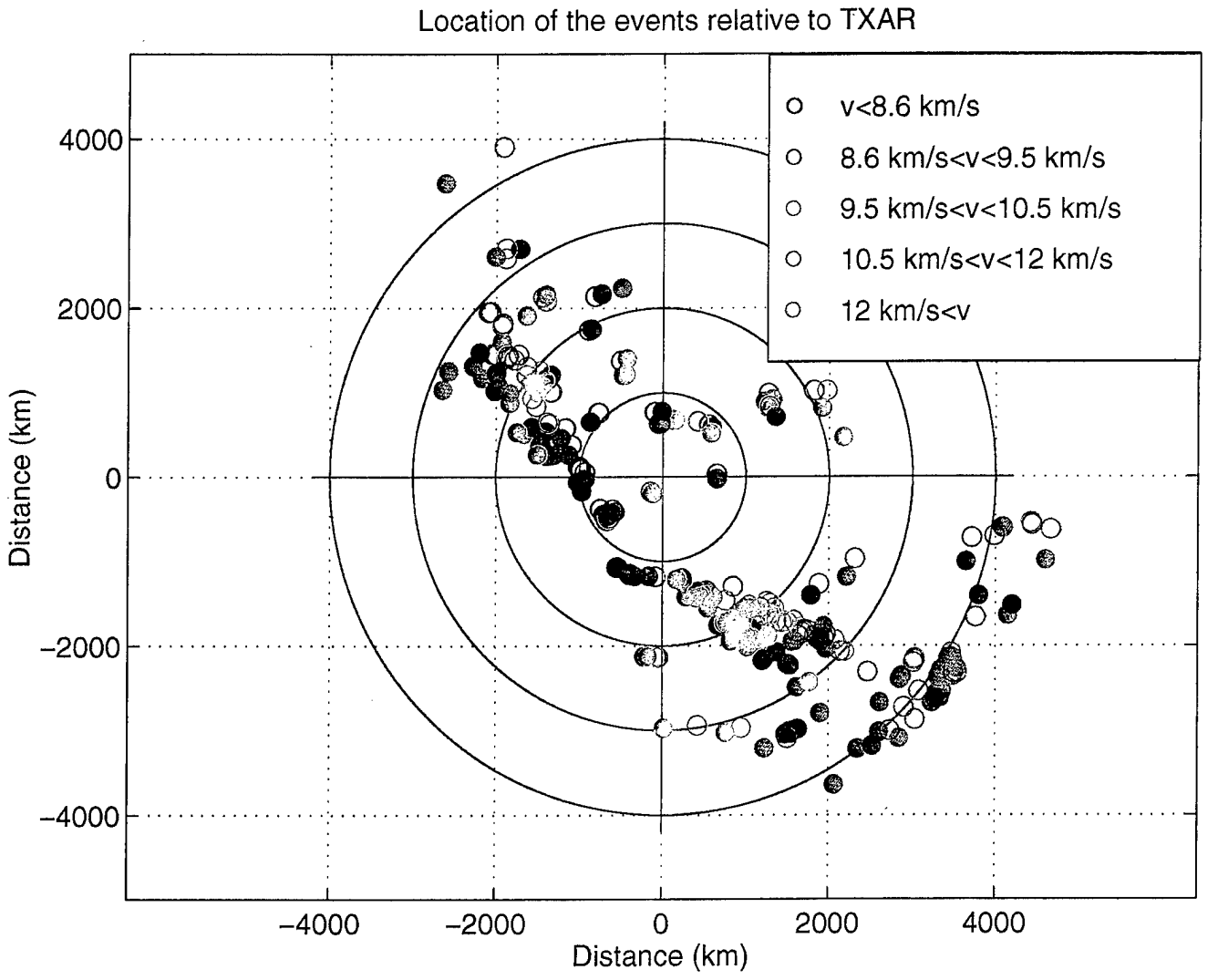

Figure 4. Representative locations of the events relative to TXAR. Open circles represent the true azimuth (USGS), solid circles represent the estimated azimuth (TXAR)

within the array and then median values were used to estimate the elements of the Toeplitz matrix. An iterative method that minimizes the L1 norm (minimum absolute deviation) was used to estimate back-azimuth and horizontal phase velocity using the elements of the estimated matrix. The L1 method was preferred to the minimization of a L2 norm because the L1 solution is more stable for data sets in which the errors are not Gaussian-distributed. The window was then moved 0.125 sec and the correlation process repeated. Using estimates of horizontal phase velocity and back-azimuth and the normalized sum of the absolute errors of the fit plotted as a function of the window start time, a 'best' window was selected based on stability of estimates and minimum estimation error. The array beam was computed using the lags for the 'best' window.

The maximum zero-to-peak amplitude and the corresponding period were measured for the first arrival of each event and the following formulas were used to estimate the magnitude:

1. Evernden (1967) formulas:

$m_{7.9} = -7.55 + 1.21 (\log (A/T) + 3.04 \log d)$ for P_n group velocity of 7.7-7.9 km/s,

$m_{8.1} = -17 + 7 \log d + \log (A/T)$ for P_n group velocity of 8.0 - 8.1 km/s,

where A is the maximum amplitude zero-to-peak in nm, d is the epicentral distance in km, T is the corresponding period in seconds.

2. Richter (1958) formula:

$m_R = \log (A/T) + Q$

where A is the maximum amplitude zero-to-peak in microns, T is the corresponding period in seconds and Q is a factor including the station correction summed with a quantity read from the contours on charts for the given phase, distance and depth.

3. Veith and Clawson (1972) formula:

$m_p = \log (A/T) + P$

where A is the peak-to-peak short period vertical P-wave amplitude in nm, T is the corresponding period in seconds and P are tabulated correction factors depending on distance and depth.

4. Denny, Taylor and Vergino (1987) formula:

$m_D = \log(A) + 2.4 \log d - 3.95 + C$

where A is the maximum amplitude (zero-to-peak) in nm, d is the epicentral distance in km and C is a constant to be determined for each station.

2.5 DISCUSSION

Corrected phase velocities normally associated with P_n (less than 8.6 km/s) are seen for events with epicentral distances less than about 2000 km. Upper mantle first arrivals (see Figure 2-1) with corrected phase velocities less than 9.5 km/s and greater than 8.6 km/s are observed generally for epicentral distances beyond 1600 km and less than 2500 km. The pattern of corrected phase velocities versus distance is not symmetrical for distances less than 1600 km. Signals coming from the western United States (NW of TXAR) travel more slowly than those coming from the same distance SE of TXAR (Mexico and Central America).

2.6 REPRESENTATIVE EVENTS

The azimuth and horizontal phase velocity corrections were calculated for regional and teleseismic events and are not applicable to local events. Estimates of phase velocity and azimuth have been made for the five events in Table 1. They are considered to be representative of events studied. Back-azimuth residuals as large as 14 degrees were found for the April 14, 1995, Alpine, Texas, earthquake, where P* is the first arrival at TXAR. This residual implies that the crustal layers beneath TXAR are also dipping to the SW and that a correction for back-azimuth and velocity should be calculated specifically for local events (see Figure 4).

Table 1 -- Representative Events

Location	Date	Origin Time	Mag	Dist (km)	Az (deg)	
					True	Est
Oklahoma	1/18/95	15:51:37	m_b(Lg)=4.0	823.3	42	45
Mexico	2/14/95	10:20:46	m_b=4.3	1887.3	145.8	156
Galapagos	6/18/95	03:42:09	m_b=5.0	3120.4	162.2	165.8
California	9/1/94	15:15:52	m_b=6.6	2343.2	307	302
Texas	4/14/95	00:32:54	m_b=5.8	107	18	4

These events are shown in Figures 5 through 9. Subplots 1 at the top represents the filtered beam and the 3.2-seconds window used to form the beam. Subplots 2 & 3 in the middle show the waveforms parameters: horizontal phase velocity and back-azimuth function of the beginning time of the 3.2 seconds window. Subplots 4 at the bottom shows the sum of the time residuals as a function of the beginning time of the 3.2 seconds window. The location of the left part of the window is marked.

The Oklahoma event shown in Figure 5 belongs to the category of weak regional events. For a 2-sec interval after the first arrival enters the window, the low frequency filtered waveforms show stable velocity and back-azimuth and a low sum of absolute deviations divided by n-2. P_n (corrected velocity 7.6 km/s) is the first arrival. For some back-azimuths, such as the one for this event, the estimated back-azimuth is within a couple of degrees of the USGS back-azimuth from TXAR because the direction of propagation is almost perpendicular to the strike of the dipping M-discontinuity.

A Mexican event, off the coast of Chiapas, is shown in Figure 6. This is an example of a small teleseismic event with a P_n (corrected velocity 8.1 km/s) first arrival followed by a mantle P wave (corrected velocity 9.3 km/s). Back-azimuth residuals as large as 15 degrees and small phase velocity residuals are observed for waves coming from this direction that is nearly along the strike of the M-discontinuity.

Figure 7 shows a teleseismic event from the Galapagos Islands Region with a good signal to noise ratio and a clear mantle P arrival (corrected velocity 10.3 km/s). The estimated back-azimuth is very close to the true back-azimuth.

A California event, off the coast of Cape Mendocino, is shown in Figure 8. This was a large teleseismic event with a mantle P wave (corrected horizontal velocity 12.4 km/s) as a first arrival. The pronounced oscillations in horizontal phase velocity and back-azimuth around a stable value that occur for this event as well as for other teleseismic events with high signal-to-noise ratio are considered to be the effect of successive entrances of the signal at each channel of the array into the moving window. Corresponding to the number of channels with signal contained in the window at a certain

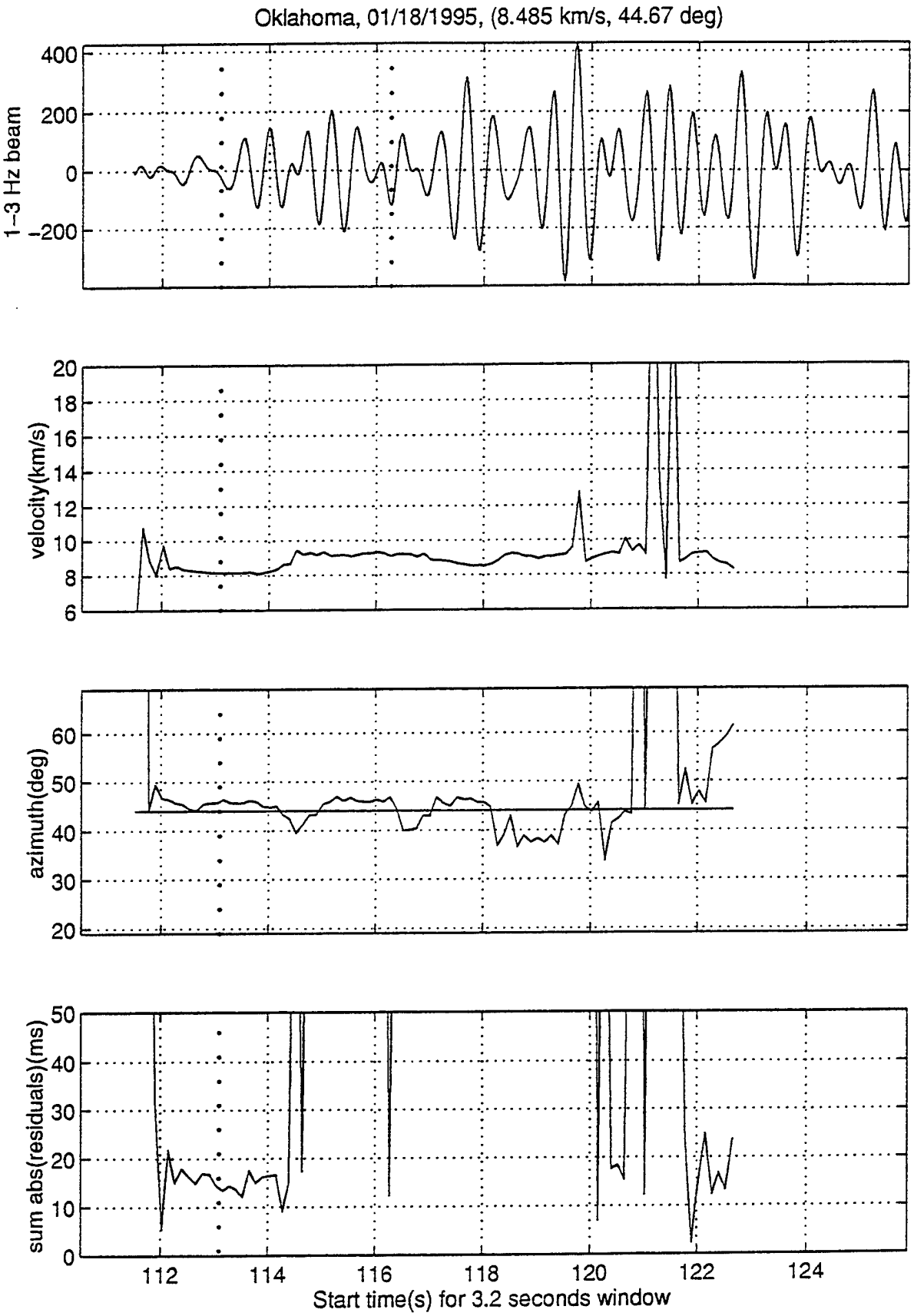

Figure 5. Oklahoma event of 18 January 1995.

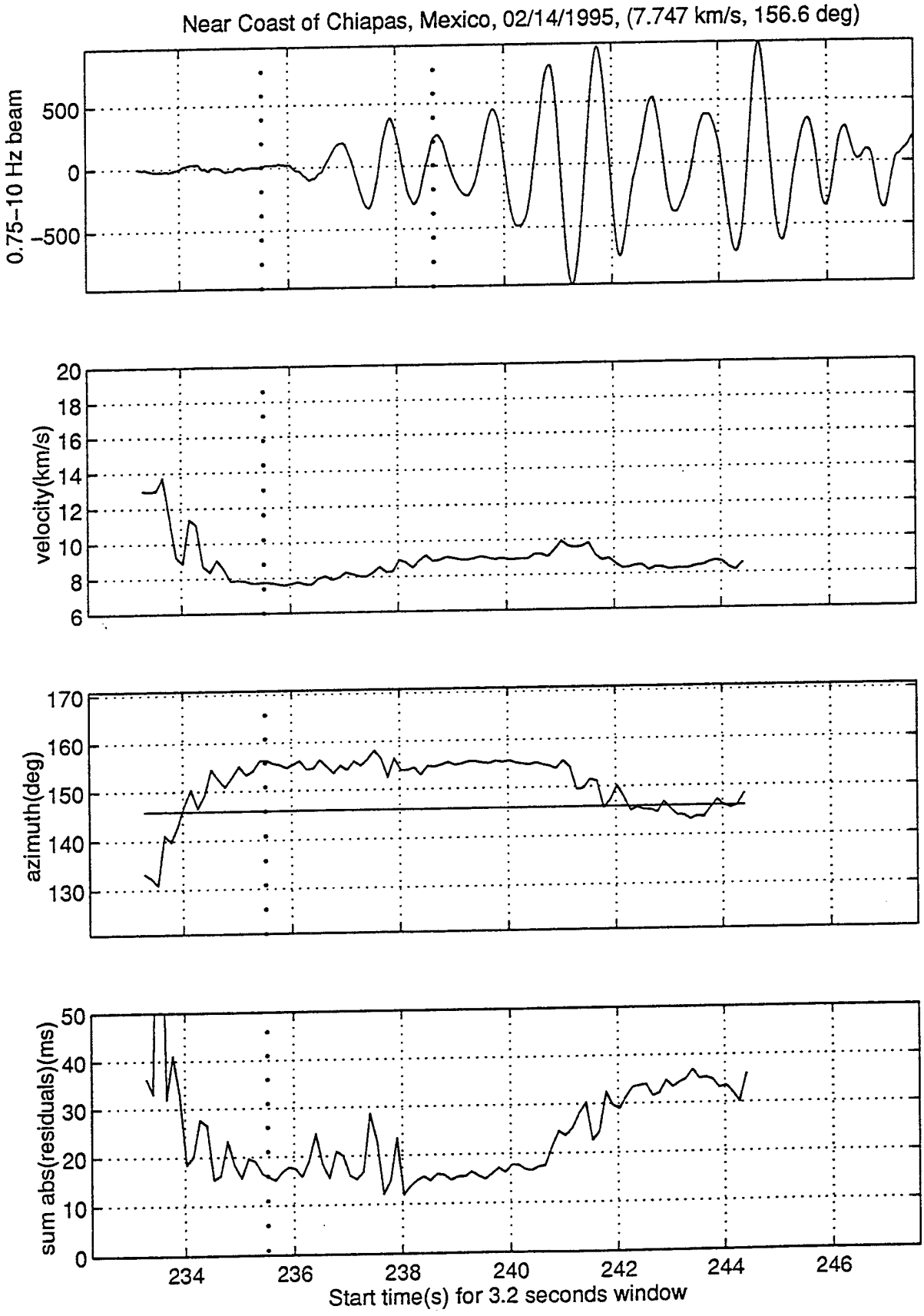

Figure 6. Mexican event of 14 February 1995

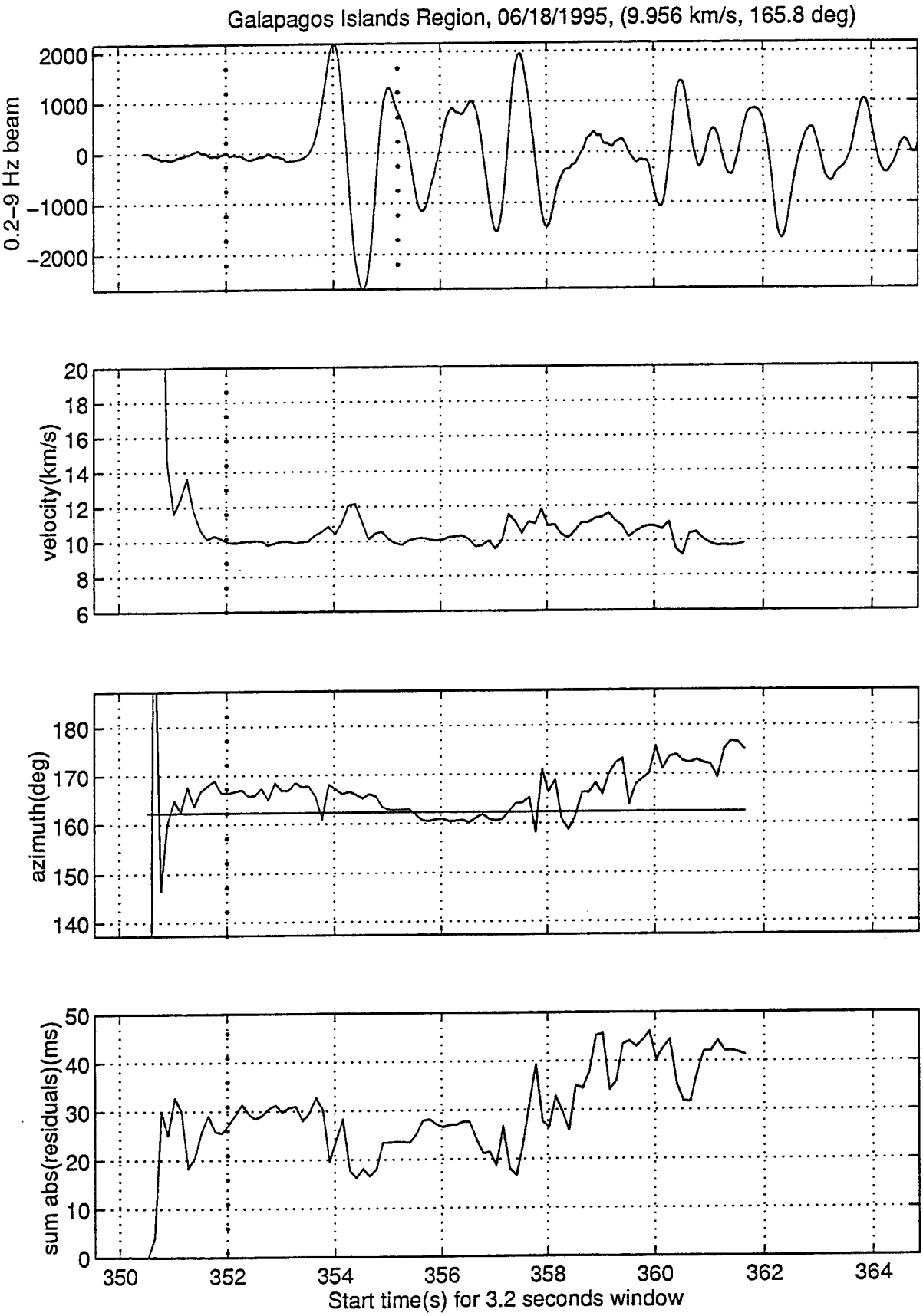

Figure 7. Galapagos event of 18 June 1995

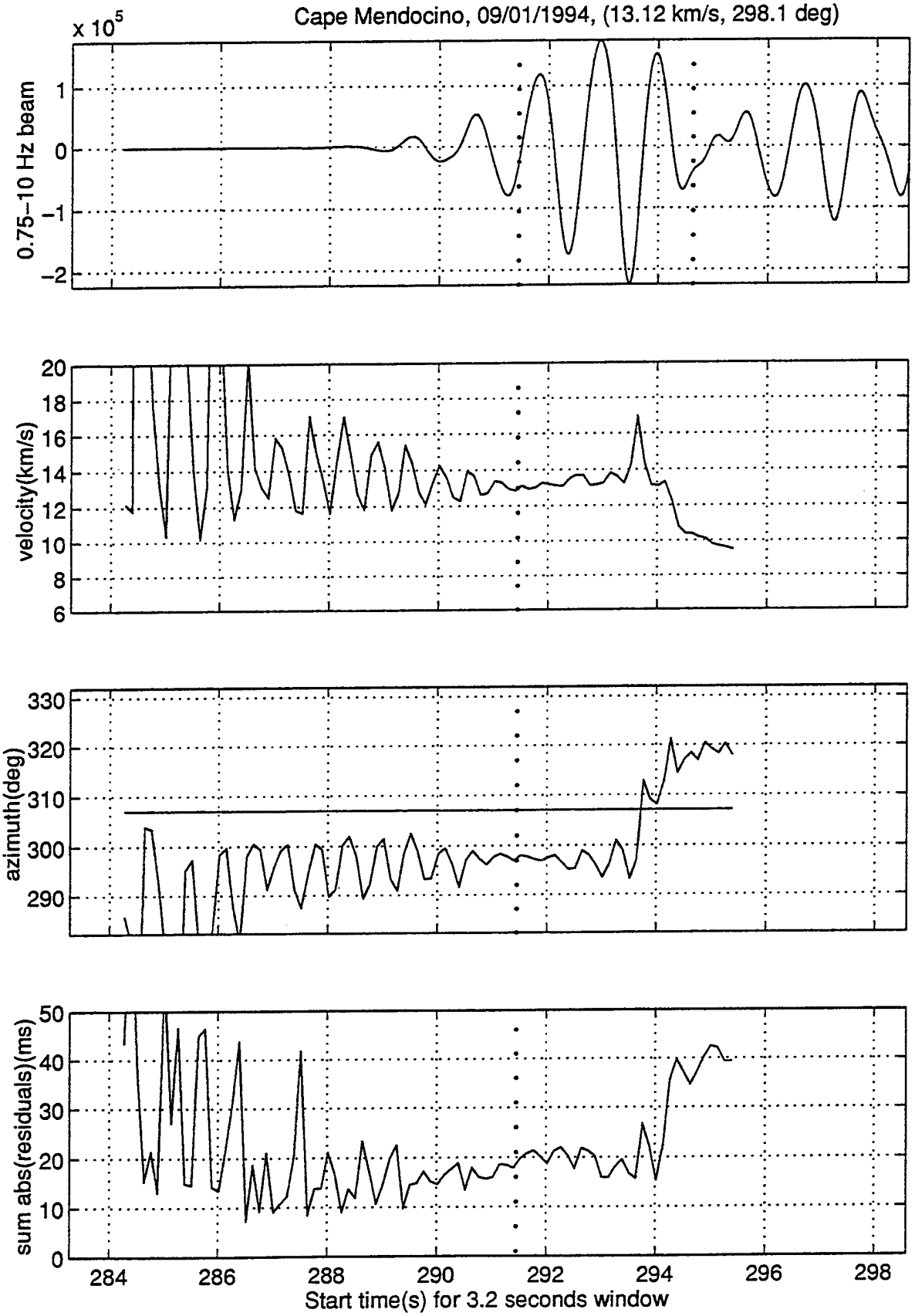

Figure 8. California event of 1 September 1994

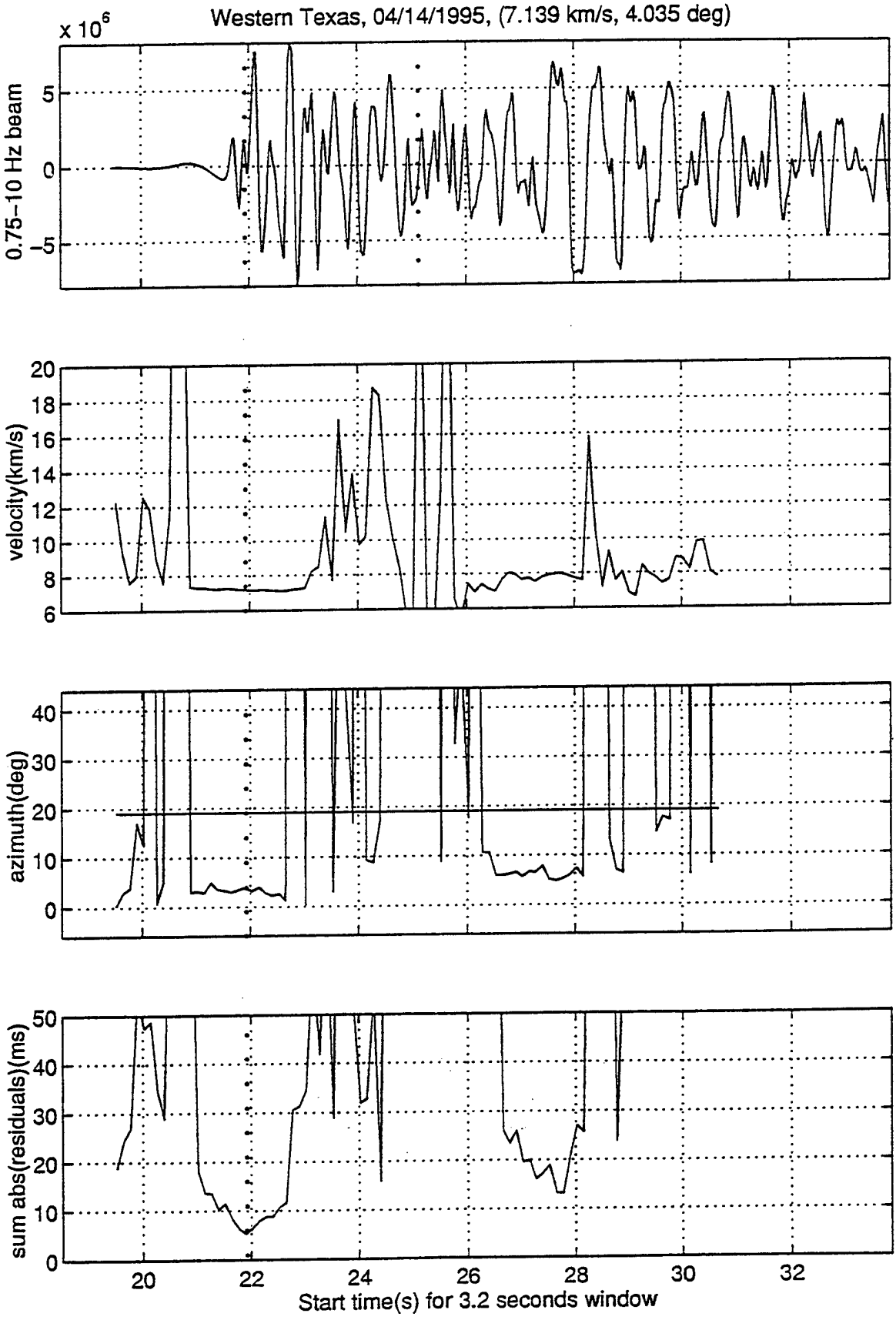

Figure 9. Texas event of 14 April 1995

moment, the peak of the cross-correlation function is shifted resulting in the oscillations. Stable values of the parameters are obtained when arrivals at all channels are well within the window. The oscillations also reappear at the transition between two successive phases. Values of the back-azimuth residuals as large as 15 degrees were observed for arrivals coming from this direction.

The Texas event, which was located about 100 kilometers north of TXAR in the Glass Mountains near Alpine, is shown in Figure 9. It is a large local event with a P* (uncorrected phase velocity 7.1 km/s) as a first arrival. The digitally clipped data from channel TX02 are presented in Figure 10. The correlation method used in this study gives stable back azimuth and horizontal phase velocity estimates even for digitally clipped data. The arrival of Pn occurs at time mark 26 in Figure 10.

The back-azimuth residuals and the horizontal phase velocity residuals versus the estimated azimuth are presented in the upper plots of Figure 11 and 12 respectively, together with the L1 cosine fit curves. We found no significant dependence of the residuals upon distance out to about 4700 km. The strike of the dipping crust-mantle boundary was found to be the point with the largest azimuth residual following the first zero crossing of the cosine fitting curve in Figure 11. Following the rule used also by Niazi (1966) that, if the azimuths are read clockwise, the direction of the dip is given by the point of transition of the azimuth residuals from negative to positive values, the direction for the dip under TXAR was determined to be to the NE. The velocity residuals have an asymmetric cosine shape, and their values should be close to zero for rays coming along strike and maximum in absolute value for rays coming up-dip or down-dip. Using theoretical azimuth and velocity residuals, curves calculated for an incidence angle of 40 degrees for the P wave at the mantle-crust boundary were the best fit to the experimental curves considering that a strike of 111 degrees NW - SE was obtained for a dip angle of 10 degrees. The second plot in each of Figures 11 and 12 shows the corrected residuals of back-azimuth and horizontal phase velocity.

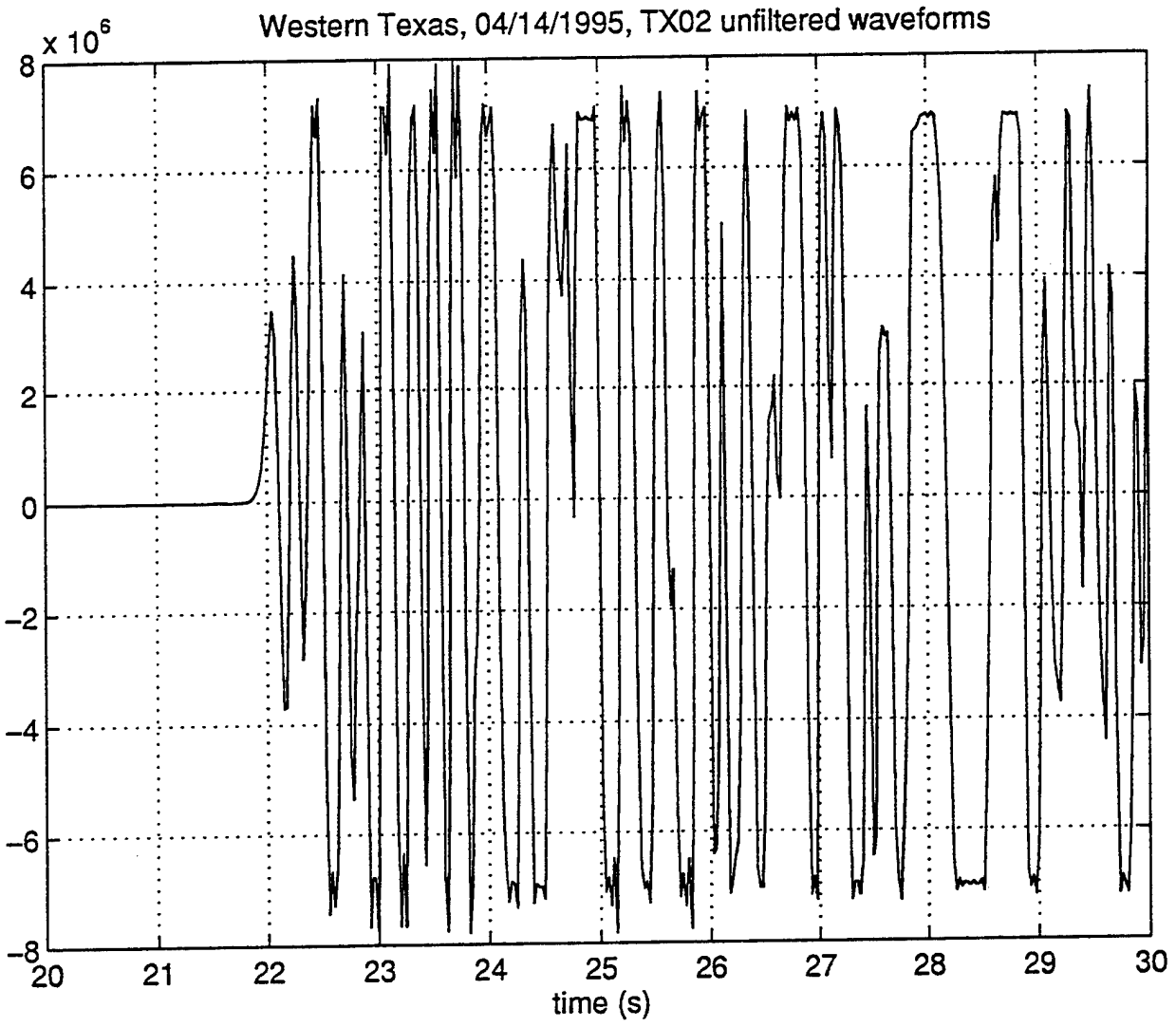

Figure 10. Digitally clipped data from the Texas event 107 km north of TXAR.

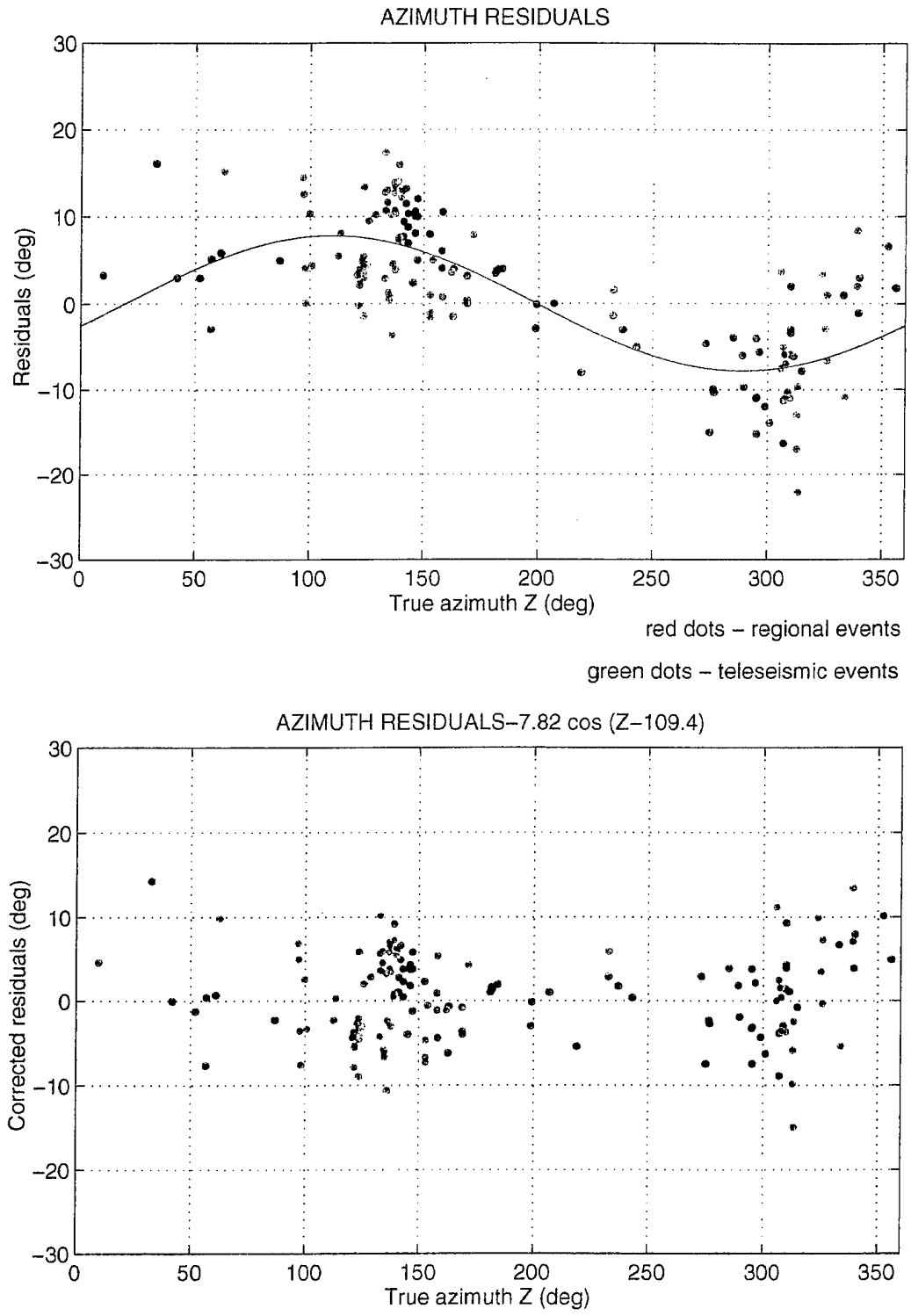

Figure 11. Azimuth residual plots. Subplot 1 shows the back-azimuth residuals (estimated TXAR back-azimuth - true USGS back-azimuth) versus the estimated back-azimuth in degrees and a best L1 fit curve. Red dots represent regional events, green dots represent teleseismic events. Subplot 2 shows the corrected back-azimuth residuals, mean = 0.7 degrees, standard error = 5.3 degrees.

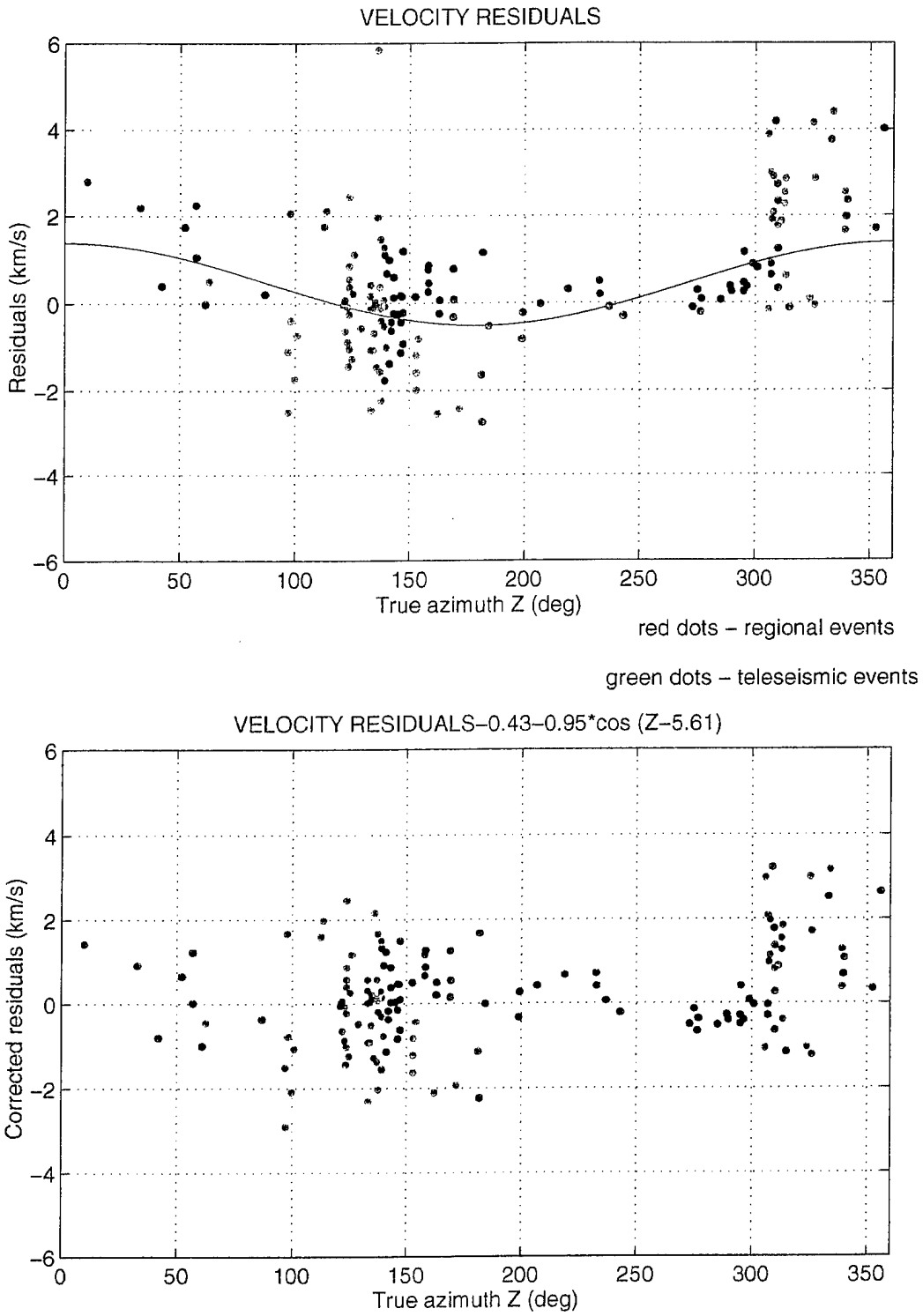

Figure 12. Phase velocity residuals. Subplot 1 shows the phase velocity residuals in km/s (estimated TXAR phase velocity - true iasp91 phase velocity) versus the estimated back-azimuth in degrees and a best L1 fit curve.Subplot 2 shors the corrected phase velocity residuals, mean = 0.3 km/s, standard error = 1.2 km/s.

2.7 CONCLUSIONS

Based on the 144 well located events (USGS), to the first order, the M-discontinuity beneath TXAR was determined to have a strike azimuth of 111 degrees (NW - SE) and to dip 10 degrees NE. The result is consistent with the tectonic setting for the area where the southern part of the Rio Grande Rift near TXAR corresponds to the direction of the strike and the crust is assumed to thin in the SW direction into the rift zone. This structure leads to bias in estimates of back-azimuth and horizontal phase velocity using TXAR data. The following corrections should be made to the estimates:

1. Azimuth correction (dZ): add to the estimated back-azimuth Z in degrees

$$dZ = -7.44 \cos (Z - 111.2)$$

2. Phase velocity correction (dV): add to the estimated phase velocity (V) in order to correct to the IASPI standard model

$$dV = -[0.44 + 0.86 \cos (Z + 0.12)]$$

The formula proposed by Denny, Taylor and Vergino (1987), provided magnitude estimates with the lowest standard deviation relative to the m_b (USGS), therefore it was chosen to estimate the magnitude.

The regional and teleseismic magnitude formulas for TXAR calibrated to m_b (USGS) are as follows:

For corrected phase velocity less than 8.6 km/sec used:

$$m = \log A + 2.4 \log d - 3.95 + C \text{ with } C = + 0.29$$

For corrected phase velocity 8.6 or greater:

$$m = \log A + 2.4 \log d - 3.95 \text{ with } C = - 0.5$$

where A is max. 0 - P amplitude in nanometers in the first 5 seconds and d is the epicentral distance in km.

The version of the correlation method used in this study allows the analysis of weak regional to teleseismic events (2.7 minimum magnitude) and the identification of successive phases for each event. Corrected phase velocities show that P_n first arrivals come to TXAR from as far as about 2000 km. All events at greater distances have mantle P waves as first arrivals. Corrected

back-azimuth residuals have a standard deviation of 5.3 degrees and a mean of 0.7 degrees and corrected phase velocity residuals have a mean of 0.3 km/s and a standard deviation of 1.2 km/s based on the NEIS locations and the iasp91 model. Using the two formulas proposed to calibrate the TXAR magnitudes to m_b (USGS), we found for both distance ranges a standard deviation of 0.6 magnitude units relative to the USGS values.

2.8 REFERENCES

Evernden, J. F., 1967, Magnitude determination at regional and near-regional distances in the United States: Seis. Soc. Am., **57** (4), 591-639.

Cansi, Y, Plantet, J. L., Massinon, B., 1993, Earthquake location applied to a mini-array: K- Spectrum versus correlation method: Geophys. Res. Lett., **20**, (17), 1819-1822.

Denny, M. D., Taylor, S.R., Vergino, E.S., 1987, Investigation of m_b and M_S formulas for the Western United States and their impact on the Ms/m_b discriminant: Seis. Soc. Am, **77** (3), 987-995.

E. Herrin, J. Taggart, (1962), Regional variations in P_n velocity and their effect on the location of epicenters: Seis. Soc. Am., **52** (5), 1037-1046.

IASPEI 1991 Seismological Tables, 1991, edited by B.L.N Kennet, Research School of Earth Sciences, Australian National University, 166-167.

Niazi, M., 1966, Corrections to apparent azimuths and travel-time residuals for a dipping Mohorovicic discontinuity: Seis. Soc.Am, **56**, (2), 491-509.

Otsuka, M., 1966a, Azimuth and slowness anomalies of seismic waves measured on the Central California Seismographic Array. Part I. Observations: Seis. Soc.Am, **56** (1), 223-239.

Otsuka, M., 1966b, Azimuth and slowness anomalies of seismic waves measured on the Central California seismographic array. Part II. Interpretation: Seis. Soc.Am, **56** (3), 655-675.

Richter, C. F., 1958, Elementary Seismology: W. H. Freeman & Co., 685-688.

Veith, K. F. and Clawson, G. E., 1972, Magnitude from short period P-wave data: Seis. Soc. Am. **6** (2), 435-452.

3. GROUND TRUTH DATABASE

G. G. Sorrells and Eugene Herrin

3.1 INTRODUCTION

Data from TXAR is being used to construct a new Ground Truth Data Base (GTDB) using regional events from a variety of sources. We are considering the development of a database appropriate for seismic sources and propagation conditions in regions other than central Europe, particularly North Africa and the Middle East. During GSETT2, over 900 regional events were observed by the three-component station at Lajitas and reported to the IDC's during a six week period. Because we have no reason to believe that the seismic activity in the region was unusual during that period, we can predict that the TXAR array will observe up to 8000 regional events per year. Known sources for these events include mine explosions, normal earthquakes, earthquake swarms, probably associated with the southward extension of the Rio Grande Rift, and very shallow earthquakes induced by the production of hydrocarbons. These induced earthquakes are only 1 to 4 km deep and have been observed with magnitudes ranging from 1.0 to 4.6. We believe that all of the events in the Permian Basin of Texas to the northeast of TEXESS are induced and are associated with oil and gas fields. We predict that TEXESS will record several hundred induced events per year from this basin.

No discriminant has yet been tested using a GTDB which includes earthquakes induced by hydrocarbon production, but events of this kind are surely occurring in the oil and gas fields of North Africa and the Middle East (see Bou-Rabee and Talwani, 1993). A GTDB which includes all of the above mentioned sources will be constructed and verified by field observation as required. Our laboratory has fifteen portable, digital seismic stations which can be used in this study.

The GTDB constructed form TXAR data (16 Hz bandwidth) will be provided to the Center for Monitoring Research in CSS 3.0 format and will be available for testing all proposed regional discriminants. After the planned ARPA

Model 94 regional array is installed by SMU personnel in Egypt, we will add data from events in North Africa and the Middle East to the CSS data base.

3.2 SEISMO-ACOUSTIC CORRELATION DETECTION OF SHORT PERIOD ACOUSTIC SIGNALS AT TXAR

The results presented in "A Preliminary Investigation Of The Use Of Acoustic And Seismo-Acoustic Observations To Identify Vented Explosive Seismic Sources," Scientific Report No. 6, demonstrate that short period acoustic and seismo-acoustic signals share a common waveform at TXAR. Furthermore, as indicated by the coherence estimates shown in Figure 8 of that report, short period seismic and infrasonic noise at frequencies greater than 1 hertz may be considered to be statistically independent processes under both calm and windy atmospheric conditions. Therefore, a running estimate of the normalized correlation coefficient for simultaneously acquired seismic and infrasonic data sets from collocated sensors should provide a simple and effective method for the detection of short period acoustic signals at TXAR.

A MATLAB code has been written to estimate the normalized correlation coefficient between two input data records. In its current configuration, the code accepts records of selectable lengths from the outputs of the collocated TX01 short-period vertical seismograph and pressure transducer. The records are filtered to account for differences in nominal sensor system responses and to pass data in the 2-8 hertz bandwidth. Estimates of the normalized correlation coefficient are currently made in a 5 second window which is sequentially shifted forward in one second intervals. The output of the code is a time series whose amplitudes are found in the interval **[-1,1]** and whose sample points are separated by 1 second in input record time. The values of this time series are expected to cluster near zero when both data records contain noise only and to be greater than zero when the records contain acoustic and seismo-acoustic signals plus noise. This configuration has been tested by using pairs of synthetically generated, statistically independent, normally distributed data records. The objective of the test was to estimate "false alarm" probability distribution characterizing this particular correlator code configuration. The histogram showing the frequency of occurrence distribution for the synthetic sample correlation coefficients is shown in

Figure 13 a. Notice that the sample population is normally distributed with a near zero mean and a standard deviation of 0.112. An identical test was performed on real data acquired during intervals that were free of visible seismic signals. The resulting histogram showing the frequency of occurrence distribution for the real sample correlation coefficients is shown in Figure 13 b. Observe that this sample population appears to be normally distributed with a slightly positive mean. It should also be noted that the standard deviation of the sample population drawn from the real data sets is somewhat larger than the standard deviation characterizing the synthetic population. These differences are believed to indicate that naturally occurring acoustic events make a minor but statistically significant contribution to the seismic and acoustic data recorded in the 2-8 hertz passband at TXAR.

3.3 SEISMO-ACOUSTIC IDENTIFICATION OF VENTED NEAR REGIONAL EXPLOSIONS

It was argued in the introduction to this text that the detection of an acoustic signal and its association with a prior seismic event unambiguously identifies the source of both as a vented explosion. A preliminary test was undertaken to determine if this approach could be successfully applied to the identification of vented explosions in a limited sample of the population of near regional seismic events detected at TXAR. The test was conducted during a 7-week interval extending from 7 November 1995 to 10 January 1996. During this time period, 25 work-day records of the seismic data acquired at TXAR during local daylight hours (1300-2300 GMT) were reviewed to identify the arrival times of all potentially locatable near regional seismic events. The seismo-acoustic correlator code, operating in the configuration referenced above, was used to detectacoustic events. It was applied to the outputs of the collocated seismic and infrasonic sensors at TX01 in a 4-minute time period which included the arrival time of the seismic event plus at least 25 minutes for each identified event. The correlator code detection threshold was set at 0.3. Based upon the test results identified in the previous section, the corresponding probability of a false alarm is expected to be less than 0.005. If the correlator code output was found to be equal to or in excess of 0.3 at any time in a 20 minute window starting 5-minutes after the P arrival time, a

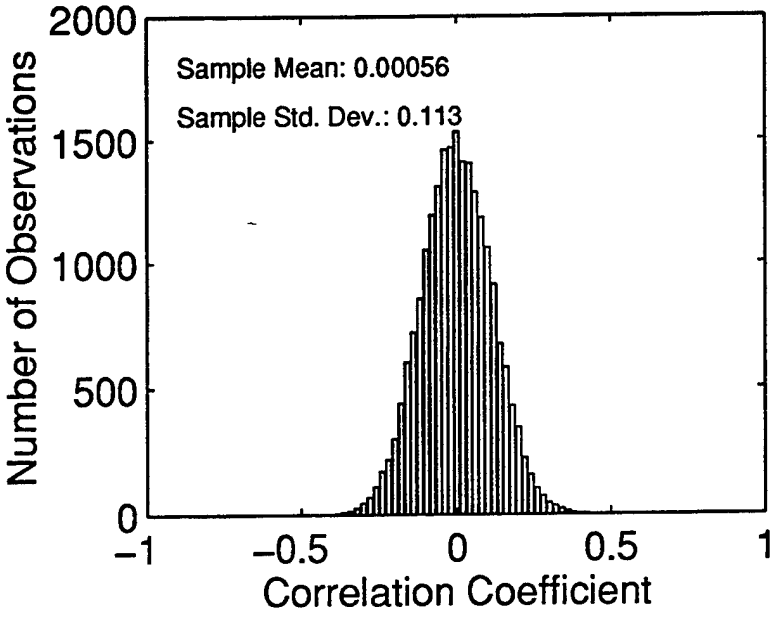

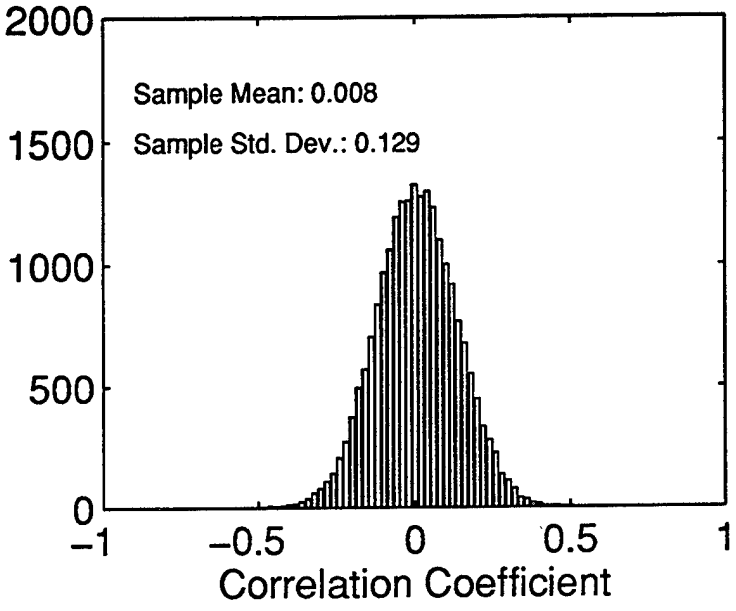

Figure 13 a. correlation code test results with synthetic data. Figure 13 b. Correlation code test results with real data.

possible associated acoustic event detection was declared and the seismic array data was analyzed to estimate the distance and azimuth to the epicenter of the seismic event and its approximate origin time. The apparent group velocity of each acoustic event detection, referenced to the epicenter and origin time of the seismic event, was then determined. If the apparent group velocity of any one of the acoustic event detections was found to lie in the interval from 0.27 km/sec to 0.33 km/sec, it was assumed to be associated with the seismic event and thus identifies the source of both as a probable vented explosion. During the 25 day test period the sources of 21 near regional seismic events were identified as probable vented explosions by the application of the procedures outlined above. A histogram of the occurrence times of these events is shown in Figure 14. Notice that their occurrence times tightly cluster near 1800 and 2100 hours (noon and 3 PM, local time). This observation strongly implies that the events are the result of industrial processes and is consistent with the identification of their sources as vented explosions. The approximate locations of their estimated epicenters are shown in Figure 15. These locations were derived from azimuth and distance estimates calculated from the array data for each event. The azimuth from TXAR to the epicenters were estimated from the P arrival time data The following equation was used to estimate the approximate epicentral distance

$$D(km)=6.22(dT + 6.5) \qquad (2)$$

where **dT** is the observed difference in the P and Lg arrival times. This equation has been found to yield reliable estimates of distances to the known epicenters of selected near regional events north and northwest of TXAR. The hachured area in Figure 15 identifies a coal mining district in northern Mexico which is thought to be a likely source of the majority of near regional events located east southeast of TXAR. If it is, then the epicentral data indicate that equation 2 significantly overestimates epicentral distances for near regional sources east of the array. In this regard, it was also found that the acoustic arrivals detected by the correlator code were systematically early when referenced to the estimated epicenters east and south of the array. Thus, pending the results of calibration studies now underway at TXAR, it is tentatively concluded that:

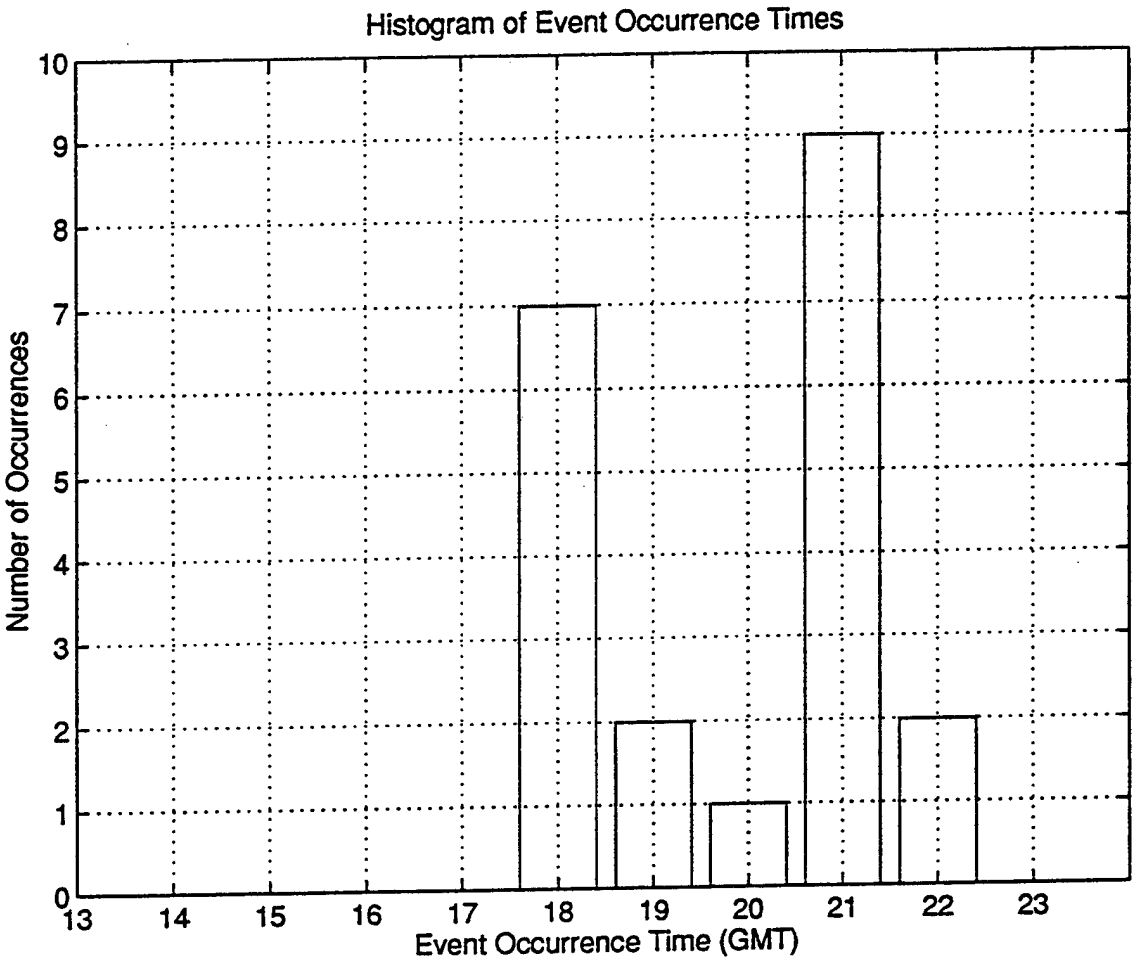

Figure 14: Histogram of occurrence times of seismic events.

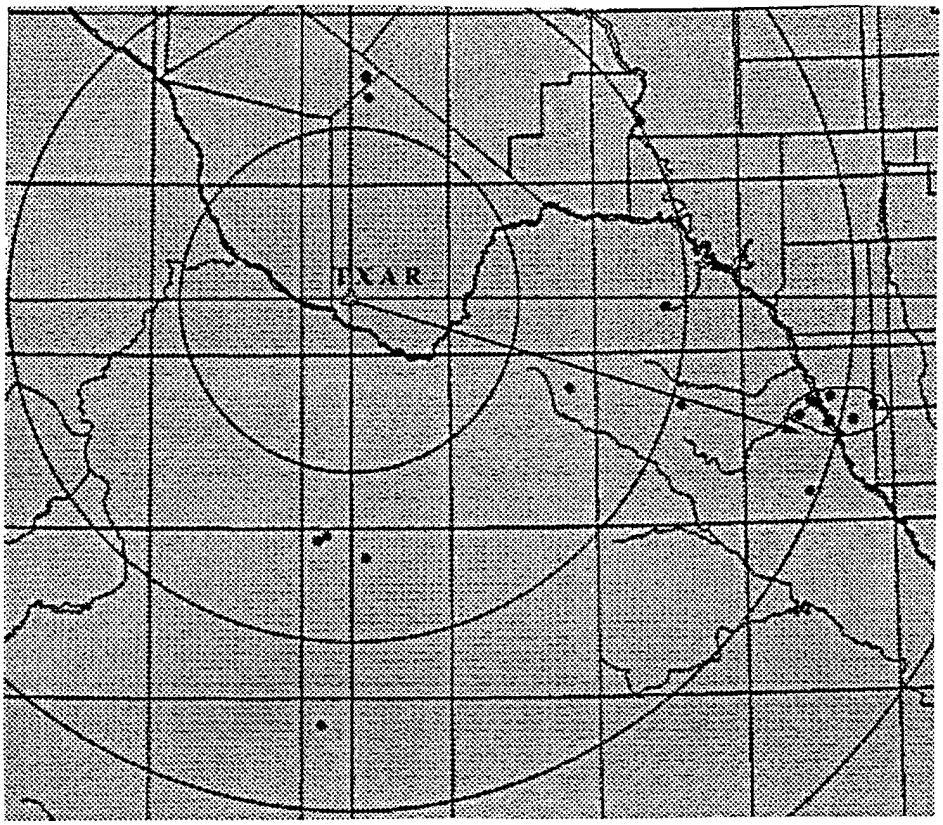

Figure 15. Location map of acoustical events recorded at TXAR.

1. At least some of the events identified as vented explosions during this test were generated in the northern Mexico coal mining district identified in Figure 15 and,

2. The use of the correlator code provides a simple but effective method for the detection of the relatively weak acoustic signals generated by near regional vented explosions.

We have tried to communicate with mine operators in the district, but they will not answer any of our questions.

3.5 SUMMARY AND CONCLUSIONS

The preliminary results of this study also demonstrate that the calculation of a running estimate of the normalized correlation coefficient between the outputs of collocated seismic and infrasonic sensors provides a simple but effective method for the detection of weak short period acoustic waves. The success of this approach at TXAR is attributed to the fact that while short period acoustic and seismo-acoustic signals share a common waveform, short period seismic and infrasonic noise are, for all practical purposes, statistically uncorrelated under both calm and windy atmospheric conditions. Statistically uncorrelated short period seismic and infrasonic noise is expected to be a property of all "hard rock" geologic environments including those which are likely to be the sites of future IMS installations. However, while acoustic and seismo-acoustic signals are always linearly related, they will share a common waveform only in those environments where the seismic velocities of the formation containing the seismic observation point are uniform over a depth range that is large compared to the wavelengths of the acoustic signals. In other environments, it will be necessary to determine the frequency response characteristics of the seismo-acoustic transfer function in order to optimize the performance of the correlator code. In this regard, it has been shown that the existing model for the prediction of seismo-acoustic transfer functions suffered from serious defects when it was tested at TXAR. Until the discrepancies between the observed and predicted values of the seismo-acoustic scaling factors at TXAR can be explained, experimental measurements should be used to determine the frequency response characteristics of local seismo-acoustic transfer functions.

3.5 REFERENCE

Bou-Rabee, P., and P. Talwani, 1993, Was the magnitude 4.7 earthquake of June 2, 1993 near Burgan oil field, Kuwait induced? *EOS Trans. AGU (Abstract)*

4. ACKNOWLEDGEMENTS

Personnel contributing to this contract are: (1) Dr. Eugene Herrin, Principal Investigator, (2) Paul Golden, Director of Geophysical Laboratory, (3) Karl Thomason, Chief Engineer, (4) Nancy Cunningham, Director - Computer Laboratory, (5) David Anderson, Systems Analyst, (6) Dyann Anderson Slosar, Administration, (7) Herbert Robertson, Subcontractor, (8) Jack Swanson, Subcontractor, and (9) Dr. Gordon G. Sorrells, Subcontractor. Ph. D. students include: (1) Chris Hayward, (2) Relu Burlacu, (3) Zenglin Cui, (4) Jessie Bonner, and (5) Ileana Tibuleac.

4.1 PREVIOUS CONTRACTS AND PUBLICATIONS

4.1.1 Previous Contracts and Reports

4.1.1.1.ARPA Contract # MDA 972-88-K-0001

Development of an Intelligent Seismic Facility and Preparation for Participation in the Conference on Disarmament Group of Scientific Experts Technical Tests (GSETT).

Quarterly R&D Status Report, 1 Nov. 1988 through 31 Jan 1989.

Quarterly R&D Status Report, 1 Feb. through 30 Apr. 1989.

Quarterly R&D Status Report, 1 May through 31 July 1989.

Quarterly R&D Status Report, 1 Aug. through 31 Oct. 1989.

Quarterly R&D Status Report, 1 Nov. 1989 through 31 Jan. 1990.

Quarterly R&D Status Report, 1 Feb. through 30 Apr. 1990.

Quarterly R&D Status Report, 1 May through 31 July 1990.

Quarterly R&D Status Report, 1 Aug. through 31 Oct. 1990: 88-K-12.

Quarterly R&D Status Report, 1 Nov. 1990 through 31 Jan. 1991.

Quarterly R&D Status Report, 1 Feb through 30 April 1991.

Quarterly R & D Status Report, 1 May through 31 July 1991.

Quarterly R & D Status Report, 1 August through 31 October 1991.

Quarterly R & D Status Report, 1 October 1991 thru 31 January 1992.

Quarterly R & D Status Report, 31 January through 30 April 1992.

Quarterly R & D Status Report, 30 April through 31 July 1992.

Quarterly R & D Status Report, 31 July through 31 October 1992.

Semiannual Report, January 1991, SMU-R-89-226.

Semiannual Report, October 1991; SMU-R-91-252

Semiannual Report, December 1991; SMU-R-91-301

Semiannual Report, January 1992; SMU-R-92-337

Semiannual Report, November 1989; SMU-R-91-121

Semiannual Report, January 1992; SMU-R-92-373

Semiannual Report, August 1992; SMU-R-92-396

Final Report, December 1992; SMU-92-425.

4.1.1.2 ARPA Contract # MDA 972-89-C-0054

Complete and Deploy the GERESS Seismic Array in Southeast Germany, Establish Workstations Which Accept the Array Data at Bochum and at NORSAR, and Provide the Interface to the Intelligent Array System at NORSAR.

Quarterly R&D Status Report, 4 Jan. to 15 Apr. 1989.

Quarterly R&D Status Report, 15 Apr. to 15 July 1989.

Quarterly R&D Status Report, 15 July to 15 Oct. 1889.

Quarterly R&D Status Report, 15 Oct. 1889 to 15 Jan. 1990.

Quarterly R&D Status Report, 15 Jan. to 15 Apr. 1990.

Quarterly R&D Status Report, 15 Apr. to 15 July 1990.

Quarterly R&D Status Report, 15 July to 15 Oct. 1890.

Quarterly R&D Status Report, 15 Oct. 1890 to 15 Jan. 1991.

Quarterly R&D Status Report, 15 Jan. to 15 April 1991.

Quarterly R & D Status Report, 15 April to 15 July 1991.

Quarterly R & D Status Report, 15 July to 15 October 1991.

Quarterly R & D Status Report, 15 October 1991 to 15 January 1992.

Quarterly R & D Status Report, 15 January to 15 April 1992.

Quarterly R & D Status Report, 15 April to 15 July 1992.

Quarterly R & D Status Report, 15 July to 15 October 1992.

Quarterly R & D Status Report, 15 October 1992 to 15 January 1993.

Quarterly Technical Report, 4 January to 15 Apr. 1989..

Quarterly Technical Report, 15 Apr. to 15 July 1989..

Quarterly Technical Report, 15 July to 15 October 1989.

Quarterly Technical Report, 15 October 1989 to 15 Jan. 1990.

Quarterly Technical Report, 15 Jan. to 15 April 1990.

Quarterly Technical Report, 15 April to 15 July. 1990.

Quarterly Technical Report, 15 July to 15 October 1990.

Quarterly Technical Report, 15 October 1990 to 15 Jan. 1991.

Quarterly Technical Report, 15 Jan. to 15 April 1991.

Quarterly Technical Report, 15 April to 15 July 1991.

Quarterly Technical Report, 15 October 1991 to 15 January 1992.

Quarterly Technical Report, 15 January to 15 April 1992.

Quarterly Technical Report, 15 April to 15 July 1992.

Quarterly Technical Report, 15 July to 15 October 1992.

4.1.1.3 Contract # 19628-93-C-0057

Design, Evaluation, and Construction of TEXESS and LUXESS, and Research in Mini-Array Technology and Use of Data from Single Stations and Sparse Networks

Quarterly R & D Status Report, 30 April to 31 July 1993.

Quarterly R & D Status Report, 31 July to 31 October 1993.

Quarterly R & D Status Report, 31 October 1993 to 31 Januaryy 1994.

Quarterly R & D Status Report, 31 January to 30 April 1994.

Quarterly R & D Status Report, 30 April to 31 July 1994.

Quarterly R & D Status Report, 31 July to 31 October 1994.

Quarterly R & D Status Report, 31 October 1994 to 31 Januaryy 1995.

Quarterly R & D Status Report, 31 January to 30 April 1995.

Quarterly R & D Status Report, 30 April to 31 July 1995.

Quarterly R & D Status Report, 31 July to 31 October 1995.

Quarterly R & D Status Report, 31 October 1995 to 31 January 1996.

Scientific Report No. 1, October 1993, PL-TR-94-2106.

Scientific Report No. 2, April 1994, PL-TR-94-2258.

Scientific Report No. 3, October 1994, PL-TR-95-2023.

Scientific Report No. 4, April 1995, PL-TR-95-2091.

Scientific Report No. 5, October 1995.

4.1.2 Publications

4.1.2.1 Special Reports, Papers, and Posters

Arnett, Dick, 1992, German Experimental Seismic System (GERESS): Pamphlet, GERESS Symposium on Regional Seismic Arrays, 22-24 June 1992, Waldkirchen, Bavaria, Federal Republic of Germany.

Bonner, Jessie, Eugene Herrin and Tom Goforth, 1995, Azimuthal variations in Rg energy in Central Texas: Appendix A, Scientific Report No. 5, 13-40, ARPA Contract # MDA 972-89-C-0054

Golden, Paul, Eugene Herrin, and Wilbur Rinehart, 1991, The use of LTX data in preparing and compiling the final event bulletins: SMU-R-91-278, Contract # MDA 972-88-K-001

Golden, Paul, 1992, Unconventional processing and visualization techniques: GERESS Symposium on Regional Seismic Arrays, 22-24 June 1992, Waldkirchen, Bavaria, Federal Republic of Germany.

Herrin, Eugene, Chris Hayward, and Eugene Smart, 1991, Comparison of the Murdock and optimum seismic signal detectors: Appendix 3, SMU-R-90-121, 54-67.

Herrin, Eugene, 1992, Construction of the GERESS array: GERESS Symposium on Regional Seismic Arrays, 22-24 June 1992, Waldkirchen, Bavaria, Federal Republic of Germany.

Herrin, Eugene and Paul Golden, 1993, Design, evaluation and construction of two nine element experimental arrays TEXESS and LUXESS: Proceedings, 15 Annual Seismic Research Symposium 8-10 September 1993, Vail, Colorado, Sponsored by Phillips Laboratory, AFOSR & ARPA, PL-TR-93-2160, ADA271458.

Herrin, Eugene, Paul Golden, Karl Thomason, and Chris Hayward, 1993, Seismic array technology: Poster.

Herrin, Eugene, 1994a, Installation of posthole 54000 seismometer, Appendix 5, Scientific Report No. 2, 59-60, ARPA Contract # MDA 972-89-C-0054.

Herrin, Eugene, 1994b, Dealing with outliers and possible evasion scenarios: Appendic A, Scientific Report No. 3, 19-35, ARPA Contract # MDA 972-89-C-0054.

Herrin, Eugene, Paul Golden and J. Theodore Cherry, 1994, The ARPA Model 94 regional array concept: Scientific Report No. 3, 36-43, ARPA Contract # MDA 972-89-C-0054.

Herrin, Eugene, *et al.*, 1994, Research in regional event discrimination using Ms:m_b and autoregressive modeling of Lg waves: Proceedings, 16 Annual Seismic Research Symposium, 7-9 September 1994, Thornwood, New York, Sponsored by Phillips Laboratory, AFOSR PL-TR-94-2217, ADA284667.

Herrin, Eugene, *et al.*, 1995, Seismo-acoustic synergy: Appendix B, Scientific Report No. 5, 41-71, ARPA Contract # MDA 972-89-C-0054.

Sorrells, G. G. and Eugene Herrin, 1995, Seismic detection of acoustical waves: Appendix B, Scientific Report No. 4, 33-42, ARPA Contract # MDA 972-89-C-0054.

Sorrells, G. G., 1995, Seismo-acoustic methods for the detection of acoustic waves: Appendix C, Scientific Report No. 5, 72-86, ARPA Contract # MDA 972-89-C-0054.

Tibuleac, Ileana and Eugene Herrin, 1996, Calibration studies at TXAR: Semiannual Report No. 1, Contract # 19628-93-C-00

4.1.2.2 Publications

Herrin, Eugene T. and Vigdor L. Teplitz, 1996, Seismic detection of nuclearites: *Physical Review D*, **53** (12), 6762-6770.

THOMAS AHRENS
SEISMOLOGICAL LABORATORY 252-21
CALIFORNIA INSTITUTE OF TECHNOLOGY
PASADENA, CA 91125

SHELTON ALEXANDER
PENNSYLVANIA STATE UNIVERSITY
DEPARTMENT OF GEOSCIENCES
537 DEIKE BUILDING
UNIVERSITY PARK, PA 16801

RICHARD BARDZELL
ACIS
DCI/ACIS
WASHINGTON, DC 20505

DOUGLAS BAUMGARDT
ENSCO INC.
5400 PORT ROYAL ROAD
SPRINGFIELD, VA 22151

WILLIAM BENSON
NAS/COS
ROOM HA372
2001 WISCONSIN AVE. NW
WASHINGTON, DC 20007

ROBERT BLANDFORD
AFTAC
1300 N. 17TH STREET
SUITE 1450
ARLINGTON, VA 22209-2308

RHETT BUTLER
IRIS
1616 N. FORT MEYER DRIVE
SUITE 1050
ARLINGTON, VA 22209

CATHERINE DE GROOT-HEDLIN
SCRIPPS INSTITUTION OF OCEANOGRAPHY
UNIVERSITY OF CALIFORNIA, SAN DIEGO
INSTITUTE OF GEOPHYSICS AND PLANETARY PHYSICS
LA JOLLA, CA 92093

SEAN DORAN
ACIS
DCI/ACIS
WASHINGTON , DC 20505

RICHARD J. FANTEL
BUREAU OF MINES
DEPT OF INTERIOR, BLDG 20
DENVER FEDERAL CENTER
DENVER, CO 80225

RALPH ALEWINE
NTPO
1901 N. MOORE STREET, SUITE 609
ARLINGTON, VA 22209

MUAWIA BARAZANGI
INSTITUTE FOR THE STUDY OF THE CONTINENTS
3126 SNEE HALL
CORNELL UNIVERSITY
ITHACA, NY 14853

T.G. BARKER
MAXWELL TECHNOLOGIES
P.O. BOX 23558
SAN DIEGO, CA 92123

THERON J. BENNETT
MAXWELL TECHNOLOGIES
11800 SUNRISE VALLEY DRIVE SUITE 1212
RESTON, VA 22091

JONATHAN BERGER
UNIVERSITY OF CA, SAN DIEGO
SCRIPPS INSTITUTION OF OCEANOGRAPHY IGPP, 0225
9500 GILMAN DRIVE
LA JOLLA, CA 92093-0225

STEVEN BRATT
NTPO
1901 N. MOORE STREET, SUITE 609
ARLINGTON, VA 22209

LESLIE A. CASEY
DOE
1000 INDEPENDENCE AVE. SW
NN-40
WASHINGTON, DC 20585-0420

STANLEY DICKINSON
AFOSR
110 DUNCAN AVENUE, SUITE B115
BOLLING AFB
WASHINGTON, D.C. 20332-001

DIANE I. DOSER
DEPARTMENT OF GEOLOGICAL SCIENCES
THE UNIVERSITY OF TEXAS AT EL PASO
EL PASO, TX 79968

JOHN FILSON
ACIS/TMG/NTT
ROOM 6T11 NHB
WASHINGTON, DC 20505

MARK D. FISK
MISSION RESEARCH CORPORATION
735 STATE STREET
P.O. DRAWER 719
SANTA BARBARA, CA 93102-0719

LORI GRANT
MULTIMAX, INC.
311C FOREST AVE. SUITE 3
PACIFIC GROVE, CA 93950

I. N. GUPTA
MULTIMAX, INC.
1441 MCCORMICK DRIVE
LARGO, MD 20774

JAMES HAYES
NSF
4201 WILSON BLVD., ROOM 785
ARLINGTON, VA 22230

MICHAEL HEDLIN
UNIVERSITY OF CALIFORNIA, SAN DIEGO
SCRIPPS INSTITUTION OF OCEANOGRAPHY IGPP, 0225
9500 GILMAN DRIVE
LA JOLLA, CA 92093-0225

EUGENE HERRIN
SOUTHERN METHODIST UNIVERSITY
DEPARTMENT OF GEOLOGICAL SCIENCES
DALLAS, TX 75275-0395

VINDELL HSU
HQ/AFTAC/TTR
1030 S. HIGHWAY A1A
PATRICK AFB, FL 32925-3002

RONG-SONG JIH
PHILLIPS LABORATORY
EARTH SCIENCES DIVISION
29 RANDOLPH ROAD
HANSCOM AFB, MA 01731-3010

LAWRENCE LIVERMORE NATIONAL LABORATORY
ATTN: TECHNICAL STAFF (PLS ROUTE)
PO BOX 808, MS L-200
LIVERMORE, CA 94551

LAWRENCE LIVERMORE NATIONAL LABORATORY
ATTN: TECHNICAL STAFF (PLS ROUTE)
PO BOX 808, MS L-221
LIVERMORE, CA 94551

ROBERT GEIL
DOE
PALAIS DES NATIONS, RM D615
GENEVA 10, SWITZERLAND

HENRY GRAY
SMU STATISTICS DEPARTMENT
P.O. BOX 750302
DALLAS, TX 75275-0302

DAVID HARKRIDER
PHILLIPS LABORATORY
EARTH SCIENCES DIVISION
29 RANDOLPH ROAD
HANSCOM AFB, MA 01731-3010

THOMAS HEARN
NEW MEXICO STATE UNIVERSITY
DEPARTMENT OF PHYSICS
LAS CRUCES, NM 88003

DONALD HELMBERGER
CALIFORNIA INSTITUTE OF TECHNOLOGY
DIVISION OF GEOLOGICAL & PLANETARY SCIENCES
SEISMOLOGICAL LABORATORY
PASADENA, CA 91125

ROBERT HERRMANN
ST. LOUIS UNIVERSITY
DEPARTMENT OF EARTH & ATMOSPHERIC SCIENCES
3507 LACLEDE AVENUE
ST. LOUIS, MO 63103

ANTHONY IANNACCHIONE
BUREAU OF MINES
COCHRANE MILL ROAD
PO BOX 18070
PITTSBURGH, PA 15236-9986

THOMAS JORDAN
MASSACHUSETTS INSTITUTE OF TECHNOLOGY
EARTH, ATMOSPHERIC & PLANETARY SCIENCES
77 MASSACHUSETTS AVENUE, 54-918
CAMBRIDGE, MA 02139

LAWRENCE LIVERMORE NATIONAL LABORATORY
ATTN: TECHNICAL STAFF (PLS ROUTE)
PO BOX 808, MS L-207
LIVERMORE, CA 94551

LAWRENCE LIVERMORE NATIONAL LABORATORY
ATTN: TECHNICAL STAFF (PLS ROUTE)
LLNL
PO BOX 808, MS L-175
LIVERMORE, CA 94551

LAWRENCE LIVERMORE NATIONAL LABORATORY
ATTN: TECHNICAL STAFF (PLS ROUTE)
PO BOX 808, MS L-208
LIVERMORE, CA 94551

LAWRENCE LIVERMORE NATIONAL LABORATORY
ATTN: TECHNICAL STAFF (PLS ROUTE)
PO BOX 808, MS L-202
LIVERMORE, CA 94551

LAWRENCE LIVERMORE NATIONAL LABORATORY
ATTN: TECHNICAL STAFF (PLS ROUTE)
PO BOX 808, MS L-195
LIVERMORE, CA 94551

LAWRENCE LIVERMORE NATIONAL LABORATORY
ATTN: TECHNICAL STAFF (PLS ROUTE)
PO BOX 808, MS L-205
LIVERMORE, CA 94551

THORNE LAY
UNIVERSITY OF CALIFORNIA, SANTA CRUZ
EARTH SCIENCES DEPARTMENT
EARTH & MARINE SCIENCE BUILDING
SANTA CRUZ, CA 95064

ANATOLI L. LEVSHIN
DEPARTMENT OF PHYSICS
UNIVERSITY OF COLORADO
CAMPUS BOX 390
BOULDER, CO 80309-0309

DONALD A. LINGER
DNA
6801 TELEGRAPH ROAD
ALEXANDRIA, VA 22310

LOS ALAMOS NATIONAL LABORATORY
ATTN: TECHNICAL STAFF (PLS ROUTE)
PO BOX 1663, MS F659
LOS ALAMOS, NM 87545

LOS ALAMOS NATIONAL LABORATORY
ATTN: TECHNICAL STAFF (PLS ROUTE)
PO BOX 1663, MS F665
LOS ALAMOS, NM 87545

LOS ALAMOS NATIONAL LABORATORY
ATTN: TECHNICAL STAFF (PLS ROUTE)
PO BOX 1663, MS D460
LOS ALAMOS, NM 87545

LOS ALAMOS NATIONAL LABORATORY
ATTN: TECHNICAL STAFF (PLS ROUTE)
PO BOX 1663, MS C335
LOS ALAMOS, NM 87545

GARY MCCARTOR
SOUTHERN METHODIST UNIVERSITY
DEPARTMENT OF PHYSICS
DALLAS, TX 75275-0395

KEITH MCLAUGHLIN
MAXWELL TECHNOLOGIES
P.O. BOX 23558
SAN DIEGO, CA 92123

BRIAN MITCHELL
DEPARTMENT OF EARTH & ATMOSPHERIC SCIENCES
ST. LOUIS UNIVERSITY
3507 LACLEDE AVENUE
ST. LOUIS, MO 63103

RICHARD MORROW
USACDA/IVI
320 21ST STREET, N.W.
WASHINGTON, DC 20451

JOHN MURPHY
MAXWELL TECHNOLOGIES
11800 SUNRISE VALLEY DRIVE SUITE 1212
RESTON, VA 22091

JAMES NI
NEW MEXICO STATE UNIVERSITY
DEPARTMENT OF PHYSICS
LAS CRUCES, NM 88003

JOHN ORCUTT
INSTITUTE OF GEOPHYSICS AND PLANETARY PHYSICS
UNIVERSITY OF CALIFORNIA, SAN DIEGO
LA JOLLA, CA 92093

PACIFIC NORTHWEST NATIONAL LABORATORY
ATTN: TECHNICAL STAFF (PLS ROUTE)
PO BOX 999, MS K6-48
RICHLAND, WA 99352

PACIFIC NORTHWEST NATIONAL LABORATORY
ATTN: TECHNICAL STAFF (PLS ROUTE)
PO BOX 999, MS K7-34
RICHLAND, WA 99352

PACIFIC NORTHWEST NATIONAL LABORATORY
ATTN: TECHNICAL STAFF (PLS ROUTE)
PO BOX 999, MS K6-40
RICHLAND, WA 99352

PACIFIC NORTHWEST NATIONAL LABORATORY
ATTN: TECHNICAL STAFF (PLS ROUTE)
PO BOX 999, MS K5-72
RICHLAND, WA 99352

PACIFIC NORTHWEST NATIONAL LABORATORY
ATTN: TECHNICAL STAFF (PLS ROUTE)
PO BOX 999, MS K5-12
RICHLAND, WA 99352

KEITH PRIESTLEY
DEPARTMENT OF EARTH SCIENCES
UNIVERSITY OF CAMBRIDGE
MADINGLEY RISE, MADINGLEY ROAD
CAMBRIDGE, CB3 OEZ UK

PAUL RICHARDS
COLUMBIA UNIVERSITY
LAMONT-DOHERTY EARTH OBSERVATORY
PALISADES, NY 10964

CHANDAN SAIKIA
WOOODWARD-CLYDE FEDERAL SERVICES
566 EL DORADO ST., SUITE 100
PASADENA, CA 91101-2560

SANDIA NATIONAL LABORATORY
ATTN: TECHNICAL STAFF (PLS ROUTE)
DEPT. 6116
MS 0750, PO BOX 5800
ALBUQUERQUE, NM 87185-0750

SANDIA NATIONAL LABORATORY
ATTN: TECHNICAL STAFF (PLS ROUTE)
DEPT. 9311
MS 1159, PO BOX 5800
ALBUQUERQUE, NM 87185-1159

SANDIA NATIONAL LABORATORY
ATTN: TECHNICAL STAFF (PLS ROUTE)
DEPT. 5736
MS 0655, PO BOX 5800
ALBUQUERQUE, NM 87185-0655

THOMAS SERENO JR.
SCIENCE APPLICATIONS INTERNATIONAL
CORPORATION
10260 CAMPUS POINT DRIVE
SAN DIEGO, CA 92121

PACIFIC NORTHWEST NATIONAL LABORATORY
ATTN: TECHNICAL STAFF (PLS ROUTE)
PO BOX 999, MS K7-22
RICHLAND, WA 99352

PACIFIC NORTHWEST NATIONAL LABORATORY
ATTN: TECHNICAL STAFF (PLS ROUTE)
PO BOX 999, MS K6-84
RICHLAND, WA 99352

FRANK PILOTTE
HQ/AFTAC/TT
1030 S. HIGHWAY A1A
PATRICK AFB, FL 32925-3002

JAY PULLI
RADIX SYSTEMS, INC.
6 TAFT COURT
ROCKVILLE, MD 20850

DAVID RUSSELL
HQ AFTAC/TTR
1030 SOUTH HIGHWAY A1A
PATRICK AFB, FL 32925-3002

SANDIA NATIONAL LABORATORY
ATTN: TECHNICAL STAFF (PLS ROUTE)
DEPT. 5704
MS 0979, PO BOX 5800
ALBUQUERQUE, NM 87185-0979

SANDIA NATIONAL LABORATORY
ATTN: TECHNICAL STAFF (PLS ROUTE)
DEPT. 5791
MS 0567, PO BOX 5800
ALBUQUERQUE, NM 87185-0567

SANDIA NATIONAL LABORATORY
ATTN: TECHNICAL STAFF (PLS ROUTE)
DEPT. 5704
MS 0655, PO BOX 5800
ALBUQUERQUE, NM 87185-0655

SANDIA NATIONAL LABORATORY
ATTN: TECHNICAL STAFF (PLS ROUTE)
DEPT. 6116
MS 0750, PO BOX 5800
ALBUQUERQUE, NM 87185-0750

AVI SHAPIRA
SEISMOLOGY DIVISION
THE INSTITUTE FOR PETROLEUM RESEARCH AND
GEOPHYSICS
P.O.B. 2286, NOLON 58122 ISRAEL

ROBERT SHUMWAY
410 MRAK HALL
DIVISION OF STATISTICS
UNIVERSITY OF CALIFORNIA
DAVIS, CA 95616-8671

DAVID SIMPSON
IRIS
1616 N. FORT MEYER DRIVE
SUITE 1050
ARLINGTON, VA 22209

BRIAN SULLIVAN
BOSTON COLLEGE
INSITUTE FOR SPACE RESEARCH
140 COMMONWEALTH AVENUE
CHESTNUT HILL, MA 02167

NAFI TOKSOZ
EARTH RESOURCES LABORATORY, M.I.T.
42 CARLTON STREET, E34-440
CAMBRIDGE, MA 02142

GREG VAN DER VINK
IRIS
1616 N. FORT MEYER DRIVE
SUITE 1050
ARLINGTON, VA 22209

TERRY WALLACE
UNIVERSITY OF ARIZONA
DEPARTMENT OF GEOSCIENCES
BUILDING #77
TUCSON, AZ 85721

JAMES WHITCOMB
NSF
NSF/ISC OPERATIONS/EAR-785
4201 WILSON BLVD., ROOM785
ARLINGTON, VA 22230

JIAKANG XIE
COLUMBIA UNIVERSITY
LAMONT DOHERTY EARTH OBSERVATORY
ROUTE 9W
PALISADES, NY 10964

OFFICE OF THE SECRETARY OF DEFENSE
DDR&E
WASHINGTON, DC 20330

TACTEC
BATTELLE MEMORIAL INSTITUTE
505 KING AVENUE
COLUMBUS, OH 43201 (FINAL REPORT)

MATTHEW SIBOL
ENSCO, INC.
445 PINEDA COURT
MELBOURNE, FL 32940

JEFFRY STEVENS
MAXWELL TECHNOLOGIES
P.O. BOX 23558
SAN DIEGO, CA 92123

DAVID THOMAS
ISEE
29100 AURORA ROAD
CLEVELAND, OH 44139

LAWRENCE TURNBULL
ACIS
DCI/ACIS
WASHINGTON, DC 20505

FRANK VERNON
UNIVERSITY OF CALIFORNIA, SAN DIEGO
SCRIPPS INSTITUTION OF OCEANOGRAPHY IGPP, 0225
9500 GILMAN DRIVE
LA JOLLA, CA 92093-0225

DANIEL WEILL
NSF
EAR-785
4201 WILSON BLVD., ROOM 785
ARLINGTON, VA 22230

RU SHAN WU
UNIVERSITY OF CALIFORNIA SANTA CRUZ
EARTH SCIENCES DEPT.
1156 HIGH STREET
SANTA CRUZ, CA 95064

JAMES E. ZOLLWEG
BOISE STATE UNIVERSITY
GEOSCIENCES DEPT.
1910 UNIVERSITY DRIVE
BOISE, ID 83725

DEFENSE TECHNICAL INFORMATION CENTER
8725 JOHN J. KINGMAN ROAD
FT BELVOIR, VA 22060-6218 (2 COPIES)

PHILLIPS LABORATORY
ATTN: XPG
29 RANDOLPH ROAD
HANSCOM AFB, MA 01731-3010

PHILLIPS LABORATORY
ATTN: GPE
29 RANDOLPH ROAD
HANSCOM AFB, MA 01731-3010

PHILLIPS LABORATORY
ATTN: PL/SUL
3550 ABERDEEN AVE SE
KIRTLAND, NM 87117-5776 (2 COPIES)

PHILLIPS LABORATORY
ATTN: TSML
5 WRIGHT STREET
HANSCOM AFB, MA 01731-3004